

239/9
4-19

1782

MASTER

Westinghouse Advanced Reactors Division



DISCLAIMER

This report was prepared as an account of work sponsored by an agency of the United States Government. Neither the United States Government nor any agency Thereof, nor any of their employees, makes any warranty, express or implied, or assumes any legal liability or responsibility for the accuracy, completeness, or usefulness of any information, apparatus, product, or process disclosed, or represents that its use would not infringe privately owned rights. Reference herein to any specific commercial product, process, or service by trade name, trademark, manufacturer, or otherwise does not necessarily constitute or imply its endorsement, recommendation, or favoring by the United States Government or any agency thereof. The views and opinions of authors expressed herein do not necessarily state or reflect those of the United States Government or any agency thereof.

DISCLAIMER

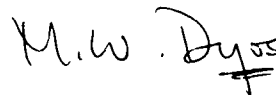
Portions of this document may be illegible in electronic image products. Images are produced from the best available original document.

EVALUATION OF ^{238}U NEUTRON CROSS SECTIONS
FOR THE ENDF/B VERSION II FILE

by

T. A. Pitterle

Approved:



M. W. Dyos
Project Manager

Prepared for the U. S. Atomic Energy Commission
Division of Reactor Development and Technology
Under Contract No. AT(30-1)4181

Submitted to AEC/NY00 in March 1971

WESTINGHOUSE ELECTRIC CORPORATION
Advanced Reactors Division
P. O. Box 158 Madison, Pennsylvania 15663

This report was prepared as an account of work sponsored by the United States Government. Neither the United States nor the United States Atomic Energy Commission, nor any of their employees, nor any of their contractors, subcontractors, or their employees, makes any warranty, express or implied, or assumes any legal liability or responsibility for the accuracy, completeness or usefulness of any information, apparatus, product or process disclosed, or represents that its use would not infringe privately owned rights.

Printed in the United States of America
Available from
National Technical Information Service
Springfield, Virginia 22151
Price: Printed Copy \$3.00; Microfiche \$0.95

ACKNOWLEDGEMENTS

The author would like to acknowledge valuable discussions with regard to the present evaluation with Dr. A. B. Smith of Argonne National Laboratory, Dr. L. Stewart of Los Alamos Scientific Laboratory, and Dr. G. Prince of Brookhaven National Laboratory and members of the ENDF/B Cross Section Evaluation Working Group Task Force for Version II evaluation. In addition, the assistance is appreciated of Dr. S. Ramchandran of the Westinghouse Advanced Reactors Division (ARD) in performing calculations quoted in this report and of Mr. F. Gallo (ARD) in obtaining graphical displays of the data.

TABLE OF CONTENTS

Chapter	Page
I	Introduction..... 1
II	Resolved and Unresolved Resonance Parameters..... 1
	A. Data Considered..... 1
	B. Resolved Resonance Energy and Momenta Assignments..... 12
	C. Resolved Neutron Widths..... 13
	D. Radiation Widths..... 13
	E. Average Resolved Resonance Parameters..... 19
	F. Unresolved Resonance Parameters..... 20
	G. Capture Cross Section and Missed Levels..... 22
III	Tabulated Pointwise Cross Section Data..... 25
	A. Cross Sections Below 5.0 eV..... 25
	B. Capture Cross Section..... 26
	C. Fission Cross Section..... 32
	D. Average Number of Neutrons per Fission - $\bar{\nu}$ 34
	E. (n,2n) Cross Section..... 34
	F. (n,3n) Cross Section..... 37
	G. Total Cross Section..... 37
	H. Nonelastic Cross Section..... 37
	I. Elastic Scattering Cross Section..... 40
IV	Inelastic Scattering Cross Sections..... 40
	A. Level Structure..... 43
	B. Resolved Levels..... 43
	C. Total Inelastic Scattering Cross Section..... 53
	D. Statistical Contribution and Nuclear Temperature..... 55
	E. Comparison of Evaluated and Measured Integral Distribu- tions..... 57
	F. Assessment of Inelastic Cross Section Accuracy..... 60
V	Conclusions..... 61
	A. Implications of Measurements Since Present Evaluation.... 61
	B. Estimates of Data Uncertainties..... 63

LIST OF FIGURES

Figure		Page
1	Comparison of Experimental and Evaluated Capture Cross Sections Between 0.1 and 10 MeV.....	27
2	Comparison of Experimental and Evaluated Ratios of ^{238}U Capture/ ^{235}U Fission.....	28
3	Comparison of Experimental and Evaluated Capture Cross Sections Between 1 and 100 keV.....	30
4	Comparison of Experimental and Evaluated Fission Ratio and of Evaluated Fission Cross Sections.....	33
5	Comparison of Experimental and Evaluated (n,2n) and (n,3n) Cross Sections.....	36
6	Comparison of Experimental and Evaluated Total Cross Sections--0.2 to 3.0 MeV.....	38
7	Comparison of Experimental and Evaluated Total Cross Sections--3.0 to 15.0 MeV.....	39
8	Comparison of Experimental and Evaluated Non-elastic Cross Sections.....	41
9	Comparison of Experimental and Evaluated Elastic Scattering Cross Sections.....	42
10	^{238}U Level Structure for Inelastic Scattering.....	44
11	Inelastic Scattering Data for 0.0447 and 0.148 MeV Levels.....	45
12	Inelastic Scattering Data for 0.310 and 0.681 MeV Levels.....	48
13	Inelastic Scattering Data for 0.732 and 0.838 MeV Levels.....	49
14	Inelastic Scattering Data for 0.939, 0.968 and 1.00 MeV Levels.....	50
15	Inelastic Scattering Data for 1.045, 1.08, 1.12, 1.17 and 1.22 MeV Levels.....	52
16	Inelastic Scattering Data for 1.27, 1.31, 1.36, 1.40 and 1.45 MeV Levels.....	54

LIST OF FIGURES (Continued)

Figure		Page
17	Comparison of Evaluated Inelastic Scattering Cross Sections.....	56

LIST OF TABLES

Table		Page
1	Experimental and Evaluated s-wave Resonance Parameters Below 210 eV.....	3
2	Experimental and Evaluated s-wave Neutron Widths Between 210 eV and 1.8 keV.....	7
3	Evaluated p-wave Resonance Parameters.....	10
4	Experimental and Evaluated Radiation Widths.....	14
5	Average Resolved Resonance Spacing and Strength Functions...	19
6	Components of Capture Cross Section and Fitted p-wave Strength Function.....	23
7	Contributions to (n, γ) Cross Section in Resolved Energy Range.....	24
8	Summary of 30 keV (n, γ) Data Used in Evaluation.....	31
9	Comparison of Experimental and Evaluated Integral Inelastic Excitation.....	58
10	Comparison of Experimental Integral Inelastic Excitation with Statistical Distributions.....	59

I. INTRODUCTION

This report describes the evaluation of ^{238}U neutron cross sections for material number 1103 of the ENDF/B Version II data file. Since the ^{238}U evaluation by Wittkopf, Roy and Livolsi [1], significant new measurements have become available for the resonance parameters, capture, fission, total and inelastic scattering cross sections. These new measurements necessitated the reevaluation of ^{238}U data described in this report.

As a result of the new measurements, all cross sections for ^{238}U have been reevaluated. Chapter II of this report describes the resonance parameter evaluation for both resolved and unresolved resonance parameters. In Chapter III, the evaluation for the capture, fission, (n,2n), (n,3n), total, nonelastic and elastic scattering cross sections are described. Chapter IV describes the inelastic scattering cross section evaluation. The implications of measurements reported since this evaluation was completed are discussed in Chapter V as well as estimated uncertainties in the evaluated data.

II. RESOLVED AND UNRESOLVED RESONANCE PARAMETERS

This chapter describes the ^{238}U evaluation for resolved and unresolved resonance parameters. The energy range for use of the resolved resonance parameters is from 5.0 eV to 3.91 keV and the unresolved energy range is from 3.91 to 45.0 keV.

A. Data Considered

The Version I ENDF/B evaluation [1] for ^{238}U resolved resonance parameters is primarily based on data from References 3 to 7 and followed the recommended data of Reference 8 below 1.78 keV and Reference 3 between 1.78 and 3.90 keV. The radiation width, Γ_γ , was taken as a constant value of 0.0246 eV. Schmidt's evaluation [9] is in general agreement with the ENDF/B evaluation although utilizing resonance dependent radiation widths for resonances for which experimental data was available. Since these

measurements, new experimental data by Asghar [10] and Glass [11] have become available and these data necessitate a reevaluation of the resonance parameters.

Asghar [10] combined capture and elastic scattering measurements, using a modified version of area analysis techniques, to obtain Γ_n and Γ_γ for 27 resonances between 6.65 eV and 823.0 eV. The weighted mean value of Γ_γ was 23.74 ± 1.09 MeV and the s-wave strength function for 46 resonances in the measured energy range was $(0.70 \pm 0.15) \times 10^{-4} \text{ eV}^{-1/2}$.

Glass [11] obtained resonance parameters by neutron time of flight utilizing the pulse source of neutrons from the Petrel nuclear explosion. Using a self-indication type measurement and analysis of the measured capture areas, radiation widths were determined for 62 resonances with an average Γ_γ of 19.1 ± 2 MeV. Approximately 200 weak resonances were examined to obtain $g \Gamma_n$ and assuming $\ell = 1$ for the weak resonances, a p-wave strength function of $(1.8 \pm 0.3) \times 10^{-4} \text{ eV}^{-1/2}$ was obtained. The neutron widths of Garg [3] were used in analyzing the capture areas to obtain the Γ_γ .

This procedure of using neutron widths from an independent measurement could lead to inconsistencies in the resulting Γ_γ and some adjustments of experimental uncertainties for the Γ_γ of Glass were made in this evaluation.

B. Resolved Resonance Energy and Momenta Assignments

Resonances found by Garg [3] and Glass [11] include a large number of small resonances which the authors assign as p-wave or doubtful resonances. The assignments of Glass are followed in this study. Thomas and Bollinger [7] performed a systematic search for p-wave resonances with low transmission dips between the large s-wave resonances. They obtained 12 resonances at 4.41, 10.25, 11.32, 19.6, 45.2, 63.6, 83.5, 93.2, 125, 153, 160 and 173 eV of which the 10.25, 153 and 173 eV were assigned $\ell = 0$ and the remaining resonances $\ell = 1$. The 10.25 eV resonance is assumed to be s-wave

in this evaluation while $\ell = 1$, following the suggestions of Glass, is assumed for the 153 and 173 eV resonances.

Resonance energies for the s-wave resonances below 210 eV were obtained as an average of the energies found in the various measurements. Above 210 eV, the resonance energies are those of Garg [3] and Glass [11] which are in generally good agreement. Resonances at 1000.3 and 1070.5 eV found by Garg but not by Glass have not been included in this evaluation. The resonance at 2631.6 eV, assigned $\ell = 0$ by Garg, has been assigned $\ell = 1$ in this evaluation following the recommendation of Schmidt [9], based on the shape and smallness of the resonance.

Resonance energies used for this evaluation are given in Table 1 for s-wave resonances below 210 eV, Table 2 for s-wave resonances between 210 eV and 1.8 keV, and Table 3 for p-wave resonances.

Table 1. Experimental and Evaluated s-wave Resonance Parameters Below 210 eV			
E(eV)	Reference	Γ_n (meV)	Γ_γ (meV)
6.65	Jackson ^[8]	1.52 ± .013	27.0 ± 1.5
6.67	Bollinger ^[17]	1.45 ± .12	26.0 ± 3.0
6.67	Lynn ^[8]	1.40 ± .1	26.1 ± 1.5
6.70	Levin ^[8]	1.54 ± .1	24.0 ± 2.0
6.70	Harvey ^[8]	1.52 ± .07	24.0 ± 2.0
6.65	Asghar ^[10]	1.58 ± .11	23.4 ± 10.1
6.67	Recommended	1.50	25.6
10.25	Thomas ^[7]	0.0015	
10.2	Bollinger ^[17]	0.0014	
10.25	Recommended	0.0015	
20.8	Bollinger ^[17]	9.9 ± .4	21.9 ± 2.3
21.0	Lynn ^[8]	8.7 ± .3	28.8 ± 2.3
21.1	Levin ^[8]	8.3 ± .7	30.0 ± 6

Table 1 (Cont'd.)			
E(eV)	Reference	Γ_n (meV)	Γ_γ (meV)
20.9	Harvey ^[8]	8.5 ± .4	25.0 ± 5
20.79	Asghar ^[10]	9.34 ± .45	33.8 ± 3.7
20.9	Recommended	8.8	26.8
36.4	Firk ^[5]	31.0 ± .9	31.3 ± 4.4
36.5	Moxon ^[6]	34.5 ± 3.0	21.2 ± 4.7
36.6	Bollinger ^[17]	34.0 ± 2.3	29.0 ± 10.0
36.8	Lynn ^[8]	28.6 ± 1.5	24.9 ± 4.2
37.1	Levin ^[8]	30 ± 4	40 ± 20
37.0	Harvey ^[8]	32.5 ± 1.9	29 ± 9
36.58	Asghar ^[10]	30.95 ± 1.17	26.3 ± 3
36.7	Glass ^[11]		20.9 ± 6.1
36.7	Recommended	31.1	26.0
66.1	Firk ^[5]	25.1 ± 1.2	25.1 ± 3.2
65.7	Moxon ^[6]	25.5 ± 1.5	24.1 ± 3.0
66.0	Bollinger ^[17]	23.4 ± 1.5	25.6 ± 9.0
66.2	Lynn ^[8]	22.6 ± 1.5	18.6 ± 4.0
66.5	Harvey ^[8]	25 ± 2	17 ± 10
65.95	Asghar ^[10]	22.7 ± .77	26.1 ± 1.7
66.3	Glass ^[11]		17.4 ± 4.6
66.1	Recommended	23.3	24.5
80.4	Moxon ^[6]	1.8 ± .3	
80.5	Bollinger ^[17]	2.1 ± .2	
81.1	Lynn ^[8]	1.8 ± .6	
81.6	Harvey ^[8]	2.1 ± .7	
80.68	Asghar ^[10]	1.85 ± .13	21.2 ± 9.0
80.8	Glass ^[11]	1.96 ± .15	
80.8	Recommended	1.88	21.2

Table 1 (Cont'd.)			
E(eV)	Reference	Γ_n (meV)	Γ_γ (meV)
89	Bollinger[17]	.084 ± .014	
90	Harvey[8]	.09 ± .03	
89.4	Glass[11]	.085 ± .01	
89.4	Recommended	.085 ± .02	
103	Firk[5]	65.9 ± 2.0	30.6 ± 6.6
101.9	Moxon[6]	69 ± 3	24.1 ± 3.0
102.8	Rosen[4]	70 ± 5	21 ± 6
102	Bollinger[17]	74 ± 5	
103.3	Lynn[8]	67.5 ± 3.0	
104	Harvey[8]	65 ± 9	
102.4	Asghar[10]	58.64 ± 1.78	25.95 ± 1.57
102.8	Glass[11]		24.9 ± 5.8
102.7	Recommended	63.0	25.5
117	Firk[5]	36.0 ± 1.5	
116.2	Moxon[6]	37.4 ± 3.5	22.1 ± 2.0
117	Rosen[4]	18 ± 3.0	21 ± 6
117	Bollinger [17]	26 ± 4	
117.5	Lynn[8]	23.2 ± 1.5	
118	Harvey[8]	15 ± 3	
116.8	Asghar[10]	23.1 ± .71	25.72 ± 1.73
116.9	Glass[11]		23.3 ± 5.6
116.9	Recommended	24.8	24.0
146	Firk[5]	.86 ± .3	
144.8	Moxon[6]	.68 ± .07	
145.9	Rosen[4]	.8 ± .2	
146	Bollinger[17]	.78 ± .27	
146	Harvey[8]	.9 ± .4	
145.7	Asghar[10]	.85 ± .064	

Table 1 (Cont'd.)

E(eV)	Reference	Γ_n (meV)	Γ_γ (meV)
145.8	Glass[11]	.84 \pm .05	
145.8	Recommended	.81	
164.4	Moxon[6]	2.8 \pm .25	
165.7	Rosen[4]	3.5 \pm .4	14 \pm 14
165	Bollinger[17]	3.1 \pm 1.1	
166	Lynn[8]	8 \pm 4	
166	Harvey[8]	2.4 \pm 1.2	
165.3	Asghar[10]	2.78 \pm .28	35.3 \pm 29.5
165.5	Glass[11]		16.2 \pm 16.2
165.3	Recommended	2.92	17.3
190	Firk[5]	150 \pm 3.0	
188.8	Moxon[6]	152 \pm 10.0	22.7 \pm 3.3
190.0	Rosen[4]	135 \pm 15.0	22 \pm 6
189	Bollinger[17]	142 \pm 14.0	
192	Harvey[8]	130 \pm 20.0	
189.7	Asghar[10]	133.2 \pm 5.1	23.21 \pm 1.72
190.3	Glass[11]		18.5 \pm 6.6
190.0	Recommended	140.0	22.8
209	Firk[5]	56 \pm 6	
207.5	Moxon[6]	57 \pm 5	23.8 \pm 4.2
209.1	Rosen[4]	55 \pm 6	26.5 \pm 4.0
208.5	Asghar[10]	50.1 \pm 1.82	21.49 \pm 1.39
208.6	Glass[11]		23.8 \pm 5.3
208.6	Recommended	51.5	22.3

Table 2. Experimental and Evaluated s-wave Neutron Widths, Γ_n^0 , Between 210 eV and 1.8 keV

E(eV)	Firk[5]	Moxon[6]	Rosen[4]	Garg[3]	Glass[11]	Asghar[10]	Γ_n^0 (meV) Recommended
237.4	2.6 ± .4	2.6 ± .4	2.1 ± .26	1.8 ± .1		1.62 ± .083	1.76
273.7			1.58 ± .17	1.52 ± .1		1.26 ± .09	1.40
291.1		.95 ± .31	1.11 ± .17	.9 ± .1		.82 ± .05	0.86
311.2			.057 ± .011	.056 ± .004	.058 ± .004	.060 ± .015	0.057
347.9	3.2 ± .5		2.95 ± .57	4.4 ± .4		3.08 ± .18	3.27
376.9	.067 ± .015	.061 ± .01	.077 ± .016	.058 ± .004	.045 ± .004	.052 ± .016	.056
397.6	.16 ± .07		.5 ± .1	.30 ± .05	.32 ± .03	.25 ± .04	.29
410.3	.40 ± .1	1.06 ± .25	.85 ± .15	.95 ± .05		.70 ± .06	.80
434.2	.15 ± .07	.78 ± .14	.67 ± .15	.40 ± .07	.50 ± .04	.38 ± .05	.42
463.4	.10 ± .04	.29 ± .04	.33 ± .10	.24 ± .02	.27 ± .015	.35 ± .05	.26
478.8	.07 ± .03	.17 ± .04	.205 ± .04	.14 ± .03		.22 ± .05	.14
518.7	2.2 ± .7	2.16 ± .44	1.63 ± .28	1.9 ± .1		1.72 ± .1	1.81
535.6	4.1 ± 1.7	4.1 ± 1.7	2.3 ± .31	1.6 ± .1		1.68 ± .11	1.68
580.2	1.08 ± .25	2.04 ± .42	1.74 ± .29	1.12 ± .03		1.56 ± .11	1.16
595.2	3.6 ± .7	3.6 ± .7	2.7 ± .42	3.35 ± .2		2.92 ± .15	3.00
620.0	.96 ± .25	1.49 ± .4	1.97 ± .32	1.14 ± .04		1.02 ± .11	1.14
628.7	.19 ± .07	.11 ± .03	.36 ± .08	.16 ± .02	.19 ± .03		0.16
661.2	7.1 ± 1.4	7.4 ± 1.6	4.85 ± .8	4.5 ± .25		4.07 ± .22	4.25
693.3	2.2 ± .6	2.28 ± .65	1.9 ± .4	1.30 ± .05		1.20 ± .13	1.25
708.5	.86 ± .2	.85 ± .2	.75 ± .15	.70 ± .1		.66 ± .12	0.73
721.8	.022 ± .011		.055 ± .011	.05 ± .01	.035 ± .006		0.04
732.3				.05 ± .005	.052 ± .007	.17 ± .05	0.052
765.1	.12 ± .06		.37 ± .12	.24 ± .04	.20 ± .03	.28 ± .06	0.24
779.1	.021 ± .007		.107 ± .02	.06 ± .005	.05 ± .007		0.06

Table 2 (Cont'd.)

E(eV)	Firk[5]	Moxon[6]	Rosen[4]	Garg[3]	Glass[11]	Asghar[10]	Γ_n^0 (meV) Recommended
790.9	.085 ± .06		.39 ± .11	.18 ± .02	.21 ± .015	.27 ± .18	0.21
821.6	2.4 ± .5		2.1 ± .35	2.05 ± .1		1.60 ± .16	1.95
851.0	3.4 ± .7		4.55 ± 1.82	1.9 ± .1			1.94
856.2	5.1 ± 1.0		2.05 ± 1.02	2.75 ± .15			2.79
866.5			.075 ± .02	.14 ± .02	.17 ± .02		0.15
905.1	1.7 ± .5		3.0 ± .7	1.5 ± .05			1.51
909.9				.03 ± .01	.043 ± .011		0.036
925.2	.98 ± .5		1.21 ± .23	.28 ± .02	.34 ± .03		0.30
936.9	4.9 ± 1.8		6.35 ± 1.27	4.8 ± .5			4.8
958.4	4.2 ± .7		6.15 ± 1.3	5.1 ± .5			5.20
991.8	11.1 ± 1.9		12.7 ± 3.0	11.0 ± .5			11.0
1011.3	.02 ± .013			.06 ± .02	.06 ± .013		.044
1023.0	.6 ± .1			.20 ± .04	.175 ± .022		.196
1029.1				.10 ± .03	.062 ± .015		.07
1053.9	1.5 ± .5			2.3 ± .5			2.1
1068.1				.02 ± .02	.031 ± .006		.03
1098.4	.21 ± .12			.45 ± .10			.35
1108.9	.17 ± .06			.90 ± .05			.80
1131.5				.06 ± .02	.11 ± .02		.085
1140.4	8.1 ± 1.1			6.5 ± .05			6.5
1167.5	1.2 ± .5			2.35 ± .15			2.26
1177.6	.9 ± .4			1.85 ± .15			1.73
1195.0	1.6 ± .5			2.65 ± .3			2.37
1210.9	.4 ± .25			.26 ± .05			.26
1245.1	6.7 ± 1.2			6.5 ± .5			6.5

Table 2 (Cont'd.)

E	Firk[5]	Moxon[6]	Rosen[4]	Garg[3]	Glass[11]	Asghar[10]	Γ_n^0 (meV) Recommended
1267.0	.7 ± .2			.75 ± .05			.75
1273.2	.8 ± .2			.80 ± .05			.80
1298.4	.28 ± .14			.08 ± .03	.11 ± .022		.10
1317.2	.29 ± .16			.11 ± .02	.12 ± .012		.12
1335.7				.03 ± .02	.047 ± .02		.039
1393.0	7.8 ± 1.6			3.7 ± .5			4.06
1405.1	2.6 ± 1.3			2.05 ± .2			2.06
1419.6	.53 ± .27			.25 ± .1	.19 ± .06		.22
1427.7	2.1 ± 1.1			.80 ± .1			.81
1444.1	.65 ± .24			.57 ± .01			.58
1473.8	2.1 ± 1.1			2.05 ± .2			2.05
1523.1	4.4 ± 1.6			5.5 ± .5			5.4
1532.0				.05 ± .02			.05
1550.0	1.3 ± .3			.03 ± .02	.076 ± .025		.048
1565.0	1.8 ± .5			.05 ± .01	.12 ± .011		.082
1598.2				8.0 ± .5			8.0 ± 0.5
1622.1	3.7 ± .7			2.10 ± .3			2.33 ± 0.5
1638.2				1.00 ± .12			1.00 ± 0.12
1662.1	2.4 ± 1.7			4.0 ± .5			3.9 ± 0.5
1688.3	1.1 ± .5			1.9 ± .3			1.7 ± 0.24
1709.4	.65 ± .32			1.35 ± .15			1.23 ± 0.24
1723.0	.48 ± .24			.33 ± .04			.34 ± 0.05
1744.0				.04 ± .01	.042 ± .06		.041 ± 0.01
1755.8	2.7 ± 1.1			1.5 ± .5			1.70 ± 0.48
1782.3	15.7 ± 2.4			11.0 ± 1.0			11.6 ± 2.0
1797.7				.05 ± .02	.061 ± .012		.058 ± 0.02

Table 3. Evaluated p-wave Resonance Parameters

E(eV)	$g\Gamma_n$ (meV)	E(eV)	$g\Gamma_n$ (meV)	E(eV)	$g\Gamma_n$ (meV)
4.41*	.00011	240.9	.063	458.4	.08
11.32	.00036	242.8 ⁺	.155	467.4	.13
19.6 ⁺	.00097	252.5	.026	485.3	.11
45.2	.0009	253.9 ⁺	.10	488.9 ⁺	.51
47.5	.0008	257.6	.03	494.6	.05
49.5	.0005	262.6	.046	499.1	.12
56.4	.0006	264.0 ⁺	.235	511.1	.10
63.5	.0052	275.3 ⁺	.16	523.6 ⁺	.27
72.8 ⁺	.010	282.5 ⁺	.13	528.2	.07
74.4	.0027	287.3 ⁺	.2	532.2	.08
83.6	.0067	294.5	.06	542.1	.16
91.0	.006	306.3	.05	550.5	.10
93.2	.0035	315.9	.05	556.0 ⁺	.75
98.2	.0048	318.6	.03	560.2	.045
111.4	.0085	322.8	.044	566.5	.033
121.4	.006	332.2	.05	585.2	.10
124.4 ⁺	.017	337.5 ⁺	.11	598.2	.11
127.4	.006	352.3 ⁺	.20	602.2	.15
133.3	.0125	354.5	.05	606.2 ⁺	.27
136.0	.006	366.4	.05	614.7	.16
137.5	.0035	373.7	.07	624.2 ⁺	.70
152.6 ⁺	.034	387.2	.04	633.1	.14
158.9	.012	395.5	.07	636.5	.12
173.0	.032	400.5	.04	664.8	.13
196.4	.015	413.5	.05	668.2	.23
200.5	.027	415.5	.05	677.0 ⁺	.85
201.5 ⁺	.038	423.0	.05	681.1	.06
215.5	.042	440.0 ⁺	.31	685.2	.06
218.8	.03	448.4	.08	688.2	.08
239.9	.053	454.4 ⁺	.44	697.5	.16

Table 3 (Cont'd.)

E(eV)	$g\Gamma_n$ (meV)	E(eV)	$g\Gamma_n$ (meV)	E(eV)	$g\Gamma_n$ (meV)
704.8	.10	1003.5	.21	1381.0	.5
711.0 ⁺	.30	1033.2 ⁺	.79	1387.4	.4
713.9	.25	1041.1	.25	1399.4	.4
716.9	.10	1047.0	.5	1410.0	.7
729.9 ⁺	.8	1063.0 ⁺	1.0	1417.0 ⁺	2.3
734.8	.15	1074.0 ⁺	.9	1422.8	.36
739.8	.09	1081.1 ⁺	1.3	1438.3	.50
743.0 ⁺	.4	1094.8 ⁺	1.5	1447.3 ⁺	1.0
756.5	.38	1102.3 ⁺	1.4	1454.8	.4
787.4	.30	1119.3	.6	1467.5	.25
797.4	.13	1150.0	.23	1482.7	.38
807.5	.33	1154.0 ⁺	.9	1488.6	.5
808.5 ⁺	.4	1158.7	.8	1494.5	.6
828.8	.4	1184.8	.2	1506.4	.6
834.8	.16	1203.0	.45	1513.3 ⁺	1.2
846.6 ⁺	.6	1218.8 ⁺	1.0	1520.2	.6
860.0	.15	1224.6	.7	1527.1	1.1
871.6	.18	1233.4	.6	1534.5	.6
881.5	.18	1236.3	.7	1539.8	.7
891.3 ⁺	.8	1251.1 ⁺	.9	1546.0 ⁺	2.6
898.2	.18	1263.0	.3	1555.8	.4
914.2	.30	1279.5	.4	1568.9 ⁺	2.0
918.2	.20	1285.4	.5	1579.6	.4
928.3	.11	1289.4	.4	1593.0 ⁺	2.0
932.5	.2	1311.7	.3	1611.6	.4
940.7 ⁺	.6	1326.0	.4	1646.8	.4
962.3	.4	1338.0	.24	1673.2	.2
965.2	.6	1347.0	.34	1682.3	.4
978.3 ⁺	.9	1363.4 ⁺	1.1	1696.3	.6
985.0	.35	1369.9	.33	1719.3	.6

Table 3 (Cont'd.)

E(eV)	$g\Gamma_n$ (meV)	E(eV)	$g\Gamma_n$ (meV)	E(eV)	$g\Gamma_n$ (meV)
1728.5	.35	2845.2 ⁺	2.7		
1735.8	.5	2908.5 ⁺	2.7		
1768.6	.5	2974.0 ⁺	2.7		
1803.5	.5	3419.0 ⁺	2.9		
1822.4 ⁺	1.1	3470.0*	1.2		
1833.5	.8	3600.0 ⁺	3.0		
1854.6	.4	3647.0 ⁺	3.0		
1866.5 ⁺	2.9	3674.0 ⁺	3.0		
1880.4	1.8	3799.7 ⁺	3.1		
1893.3	1.9				
1914.0 ⁺	3.5				
1925.2	1.6				
1933.3	.4				
1943.4	1.0				
1953.5 ⁺	4.5				
1990.3	1.2				
2000.1	.5				
2051.1 ⁺	2.0				
2194.0 ⁺	2.3				
2241.5*	1.4				
2302.0*	1.0				
2604.0 ⁺	2.6				
2631.6*	1.03				
2730.0 ⁺	2.6				
2798.0 ⁺	2.6				

⁺ Resonances included as parameters in File 2 of the ENDF/B data.

* Resonances neglected for the ENDF/B file.

Note: All resonances not indicated by + or * were included in File 3 of the ENDF/B data as pointwise cross sections calculated from the parameters.

C. Resolved Neutron Widths

Average values for the s-wave reduced neutron widths were generally obtained as averages of the various measurements with reciprocal weighting by the squares of the experimental uncertainties. For a few resonances having highly discrepant measurements, an estimate of the neutron widths was used in place of the weighted average. The s-wave data considered below 210 eV and between 210 eV and 1.8 keV are given in Tables 1 and 2 respectively. Above 1.8 keV, s-wave resonances have been measured only by Garg [3] and these results were used directly for the ENDF/B file to obtain resonances up to 3.904 keV.

Measurements for small resonances, suggested by the authors to be p-wave or uncertain resonances have been obtained by Thomas and Bollinger, Garg, and Glass with the latter providing the most extensive set of p-wave resonances up to 2.051 keV. The p-wave neutron widths evaluated from these measurements are given in Table 3.

D. Radiation Widths

All published significant measurements of the radiation widths for ^{238}U resonances are given in Tables 1 and 4. All data in these two tables have been used to obtain the weighted average in Table 4. In these tables, some adjustments of the quoted experimental uncertainties were made for the reasons given below:

1. Asghar [10] - These measurements are probably the most accurate of the extensive sets of measurements and the quoted uncertainty was obtained as the square root of the sum of the squares of the authors quoted statistical and systematic uncertainties.
2. Glass [11] - As noted in Section A, Glass could have introduced inconsistencies in his analysis by using the neutron widths of Garg [3] to analyze his measurements of capture areas for radiation widths. For this reason, these measurements were given low weighting by assigning the

Table 4. Experimental and Evaluated Radiation Widths

E(eV)	Glass [11]	Asghar [10]	Rosen [4]	Moxon [6]	Firk [5]	Weighted Average	Γ_γ (meV) Recommended
6.67		23.43 ± 10.1				25.6 ± 2.2*	25.6
20.9		33.83 ± 3.74				26.8 ± 1.9*	26.8
36.7	20.9 ± 6.1	26.33 ± 3.0		21.2 ± 4.7	31.3 ± 4.4	26.0 ± 3.3*	26.0
66.1	17.4 ± 4.6	26.07 ± 1.67		24.1 ± 3.0	25.1 ± 3.2	24.2 ± 2.2*	24.5
80.8		21.17 ± 8.98					21.2
102.7	24.9 ± 5.8	25.95 ± 1.57	21 ± 6	24.1 ± 3.0	30.6 ± 6.6	25.5 ± 1.9*	25.5
116.9	23.3 ± 5.6	25.72 ± 1.73	21 ± 6	22.1 ± 2.0		24.0 ± 2.1*	24.0
165.3	16.2 ± 16.2	35.31 ± 29.5	14 ± 14			17.3 ± 10	23.5
190.0	18.5 ± 6.6	23.21 ± 1.72	22 ± 6	22.7 ± 3.3		22.8 ± 2.3*	22.8
208.6	23.8 ± 5.3	21.49 ± 1.39	26.5 ± 4	23.8 ± 4.2		22.3 ± 1.8*	22.3
237.4	31.4 ± 7.0	19.53 ± 1.62	20.5 ± 4	24.8 ± 4.8		20.6 ± 3.0*	20.6
273.7	26.1 ± 5.2	23.91 ± 2.53	22.5 ± 3			23.7 ± 2.2*	23.7
291.1	31.4 ± 13.3	22.40 ± 2.42	19.0 ± 5			22.0 ± 4.0*	22.0
347.9	17.9 ± 3.6	20.44 ± 1.98	20.0 ± 3			19.9 ± 1.7*	19.9
397.6		37.6 ± 33.6	40.0 ± 16			39.6 ± 18	39.6
410.3	14.4 ± 2.9	26.61 ± 4.2	18.0 ± 6			18.3 ± 5	23.8
434.2		25.1 ± 8.82	20.0 ± 8			22.3 ± 5*	22.3
463.4		18.7 ± 6.0	18.0 ± 14			18.6 ± 6	18.6
478.8			35 ± 25				35.0
518.7	22.4 ± 4.5	25.12 ± 2.76	28.5 ± 4			25.4 ± 2.2*	25.4
535.6	24.9 ± 5.0	29.30 ± 3.84	24.3 ± 3			26.0 ± 2.3*	26.0
580.2	24.4 ± 6.2	22.0 ± 3.44	23 ± 3			22.8 ± 2.6*	22.8
595.2	20.8 ± 4.1	21.79 ± 2.90	23 ± 3			22.1 ± 2.0*	22.1
620.0	19.8 ± 3.9	33.10 ± 7.12	24 ± 3			23.5 ± 4	23.5
661.2	18.8 ± 3.8	25.12 ± 5.07	25.5 ± 3			23.3 ± 3*	23.3

largest of the uncertainties obtained by linear addition of the quoted statistical and systematic uncertainties or an uncertainty of 20%.

3. Moxon [6] - These measurements have not been published although reported in Reference 8 and the quoted uncertainties were increased by 50%.

4. Firk [5] - The three reported radiation widths were obtained as the difference between the Γ and the Γ_n found by area analysis of transmission data rather than by analysis of capture yields. Due to potential uncertainties in the method used for radiation widths, as possibly indicated by lack of agreement with other data for the 36.7 and 102.7 eV resonances, the quoted uncertainties were doubled for the present analysis.

Average values of the measured radiation widths for each level were obtained by reciprocal weighting by the square of the uncertainties as given in Tables 1 and 4. The resulting average values for each resonance having at least two measurements are given in Table 4.

Dependent on the procedure used to define an average radiation width, averages varying from about 19.0 to 24.5 MeV could be obtained. The average value is most sensitive to the weighting applied to the data of Glass. In Table 4 the 21 resonances having the weighted average indicated by an asterisk appear to be the most reliably determined radiation widths. For these resonances, the experimental data are generally consistent within error bounds with the weighted average. The arithmetic average of the radiation width for these 21 resonances is 23.5 MeV. Compared to all reported data, these resonances do not show large variations in Γ_γ varying from 19.8 to 26.8 MeV. The only resonances having radiation widths outside this range and supported by at least two measurements are the 397.6 and 463.7 eV resonances with averages of the Asghar and Rosen data of 39.6 ± 18 and 18.6 ± 6 MeV respectively. These two resonances have not been included in the group indicated by an asterisk due to the large uncertainties in the measurements. Inclusion of both of the resonances does not significantly alter the average of 23.5 MeV.

For 18 of the starred resonances which were measured by Glass, the average of Glass's data is 22.5 MeV compared to 23.2 MeV for the average for all measurements. This relatively close agreement for the average, however, is largely due to the two large radiation widths of 31.4 MeV found by Glass for the 237.4 and 291.1 eV resonances compared to the weighted averages of 20.6 and 22.0 MeV respectively for these two resonances. For 6 of the starred resonances, Glass found radiation widths of 20 MeV or less. Including the additional 16 measured Γ_γ up to 1 keV in the average yields 23.0 MeV. As more of the Glass data are included, the average Γ_γ decreases to 20.7 MeV for all 72 measured resonances up to 2.03 keV.

In general, the Glass data are inconsistent with the other measurements. As noted by Glass, his measurements indicate considerable structure in the radiation width as a function of energy with a tendency toward smaller radiation widths with increasing energy. In particular, Glass found that the 937 and 958 eV resonances have similar Γ_n 's but capture yields differing such that $\Gamma_\gamma(937)/\Gamma_\gamma(958) = 1.7 \pm 0.1$. The data of Rosen, although toward the upper energy limits of the measurements, yield only about a 10% difference in the capture yield for these two resonances. Other structure in Γ_γ found by Glass below 800 eV is not found in the data of Asghar or Rosen.

Based on the above considerations, the average Γ_γ was taken as 23.5 MeV for this evaluation based on the 21 resonances indicated by an asterisk in Table 4. This average is in good agreement with the weighted average of 23.7 obtained by Asghar from his data. Complete neglect of the Glass data would result in an average Γ_γ of 23.9 MeV for the 20 starred resonances below 822 eV. The recommended radiation widths below 1.0 keV are given in Table 4. Resonances above 1.0 keV and all p-wave resonances were assigned the average Γ_γ of 23.9 MeV, thus neglecting the measurements of Glass above this energy. Thus, the only consideration of the Γ_γ of Glass in this evaluation is a reduction of the average Γ_γ from 23.9 to 23.5 MeV.

Glass's Γ_γ data indicate considerable variation from resonance to resonance and an approximate tendency toward lower Γ_γ at higher energies up to the

2.0 keV upper limit of the measurements. The structure in Γ_γ found by Glass below 800 eV is not found in the data of Asghar. Glass notes that the radiation width fluctuations could be considered as arising from the total radiation widths consisting of a constant plus a fluctuating part from high energy gamma-ray transitions which vary in intensity from resonance to resonance. To test potential implications of this mechanism, statistical calculations were made using a constant $\Gamma_\gamma = 12$ MeV plus a fluctuating $\Gamma_\gamma = 11.5$ MeV having a chi-squared distribution with $\nu = 4$. It was found that this distribution leads to effects of less than 2% on infinite dilution cross sections and 1 - 10% effects on the temperature derivative (related to reactor Doppler coefficients) of the self-shielded cross sections, when compared to totally constant Γ_γ calculations. At this time, it is felt that additional verification of the magnitudes and fluctuations of the radiation widths found by Glass is required before incorporating these data into evaluated data files.

A possible mechanism for apparent fluctuations in the measured radiation widths could be random overlap of s- and p-wave resonances. Such overlap would contribute little to the neutron width of the s-wave resonance but could make a significant contribution to the measured capture area and hence the radiation width. Durston and James [12] have examined random overlap between s- and p-wave resonances in ^{238}U using a set of resonances up to 2.0 keV generated by random sampling from statistical distributions. Based on examination of the 100 s-wave and 269 p-wave resonance sample, about 20% of the p-wave resonances would be partially hidden (within 1.6 eV of an s-wave resonance as found for the closest s- and p-wave resonances in the Glass data) by s-wave resonances thus contributing to larger capture areas for the s-wave resonances. About 11% of the s-wave resonances could be mistaken for p-wave resonances or small enough to be hidden by p-wave resonances while only around 1 - 2% of the p-waves would likely be mistaken for s-waves. These effects indicate that the s-wave level spacing of 20.8 eV obtained from the resolved resonances could be overestimated by approximately 7%.

E. Average Resolved Resonance Parameters

Averages of the resolved parameters over energy intervals for level spacing $\langle D \rangle$, s-wave strength function S_0 and p-wave strength function S_1 are given in Table 5. Although the resonance assignments between s- and p-waves is somewhat arbitrary, the consistency of the s-wave level spacing indicates reasonable assignments and the average level spacing is about 20.8 eV.

ΔE keV	s-wave			p-wave		
	Number Resonances	$\langle D \rangle$	$S_0 \times 10^4$	Number Resonances	$\langle D \rangle$	$S_1 \times 10^4$ R = .84
0- .5	24	20.8		66	7.6	1.69
0-1	48	20.8		120	8.3	1.64
1-2	46	21.7		76	13.2	
2-3	48	20.8	0.84	12		
3-3.91	46	19.8	0.76	6		
0-1.5	73		0.81	163	9.2	1.48
0-2	94	21.3	0.92	196	10.2	1.36
0-3	142	21.1	0.89	208		
0-3.91	188	20.8	0.86	214		

The s-wave strength function of $0.76 \times 10^{-4} \text{ eV}^{-1/2}$ between 3.0 and 3.91 keV is considerably lower than over other intervals indicating the possibility that the neutrons widths may not be well determined in this energy range which represents the upper limit of the Garg data. An average s-wave strength function of about $0.9 \times 10^{-4} \text{ eV}^{-1/2}$ is indicated by the averages between 0-2 and 0-3 keV.

From level spacing considerations, the average value of the p-wave spacing should be about 7.4 eV or roughly one-third of the s-wave spacing. Up to 700 eV, the average p-wave resonance spacing is 7.8 eV

or less and then increases to 8.3 at 1.0 keV. Thus, below about 700 eV, most of the p-wave resonances appear to have been found. Between 5 and 10 possible missed p-wave resonances could be hidden by s-wave resonances. However, it must be emphasized that the spin assignments are not uniquely determined although they are reasonably consistent with regard to spacing and neutron width considerations.

The p-wave strength function indicated by the Table 5 data is about $1.7 \times 10^{-4} \text{ eV}^{-1/2}$ based on a neutron radius for penetrability calculations of $0.84 \times 10^{-12} \text{ cm}$. However, due to uncertainties in the p-wave assignments and large uncertainties on the small neutron width measurements, this p-wave strength function is not considered reliable and is not used in this evaluation.

In summary, the average parameters from the resolved resonance data are:

$$\begin{aligned} \langle \Gamma_\gamma \rangle &= 23.5 \text{ MeV} \\ \langle D_0 \rangle &= 20.8 \text{ eV} & S_0 &= 0.9 \times 10^{-4} \text{ eV}^{-1/2} \\ \langle D_1 \rangle &\approx 7.6 \text{ eV} & S_1 &\approx 1.7 \times 10^{-4} \text{ eV}^{-1/2} \end{aligned}$$

F. Unresolved Resonance Parameters

Unresolved resonance parameters are required within the ENDF/B file for use in resonance self-shielding calculations for reactor applications. Current ENDF/B formats permit energy variations in the strength functions in order to permit adjustment to gross structure and shape in low resolution experimental data without introduction of large negative background cross sections.

The ENDF/B format specifications [2] require that the nuclear radius for penetrability calculations be given by:

$$R = [1.23(AWRI)^{1/3} + .8] * 10^{-13} \text{ cm}$$

where AWRI is the ratio of the atomic mass to the neutron mass.

For ^{238}U

$$R = 0.84 \times 10^{-12} \text{ cm}$$

In this evaluation, the radius for the potential scattering calculation is $0.9184 \times 10^{-12} \text{ cm}$ yielding a cross section of 10.6 b. as obtained by Uttley [81].

The spin dependence of the average resonance spacing used in this evaluation is that predicted by the Fermi gas model [see References 13, 14 for example] and given by

$$\langle D \rangle \propto \frac{1}{2J + 1} \exp \left[\frac{J(J + 1)}{2\sigma^2} \right]$$

where the spin cut off parameter σ is assumed to be 4 [13]. This form yields the following low energy average spacings

$$D(\ell = 0, J = 1/2) = 20.8 \text{ eV}$$

$$D(\ell = 1, J = 1/2) = 20.8 \text{ eV}$$

$$D(\ell = 1, J = 3/2) = 11.422 \text{ eV}$$

The energy dependence of the level spacing is assumed to be of the form [13, 14]

$$\langle D \rangle \propto U^2 \exp[-2\sqrt{aU}]$$

where $U = E_n + B_n$ for a binding energy B_n of 5 MeV and a is the level density factor given by

$$a^{1/2} = \frac{A^{1/2}}{3.18} = 4.831$$

based on the value estimated from inelastic scattering nuclear temperatures (see section IV-D).

From the average resolved resonance parameters given in section E above, the greatest uncertainty is in the p-wave strength function. For this evaluation, the p-wave strength function was adjusted to fit the evaluated smooth (n,γ) cross section (see section III-B) at energies between 3.91 and 45.0 keV. This energy range was selected as it covers the energy range for which resonance self-shielding is important for fast reactor calculations. Also a cutoff at 45 keV avoids problems associated with inelastic scattering competition from the lowest level at 0.0447 MeV.

In general, d-wave contributions to the capture cross section are small below about 100 keV. However, in adjusting a p-wave strength function to fit a particular cross section, neglect of the d-wave contribution could lead to about a 10% increase in the p-wave strength function at 45 keV. Therefore, in adjusting to the evaluated capture cross section, d-waves were included based on an assumed d-wave strength function of $1.5 \times 10^{-4} \text{ eV}^{-1/2}$.

Using the average parameters, $\langle \Gamma \gamma \rangle = 23.5 \text{ MeV}$, $S_0 = 0.9 \times 10^{-4}$, $S_2 = 1.5 \times 10^{-4}$ and $D(\ell = 0, J = 1/2)$, the results of the p-wave fitting procedure are given in Table 6. Column 7 gives the p-wave strength function at each energy point obtained from fitting the evaluated capture cross section (Column 5). Columns 2 to 4 give the calculated s-, p- and d-wave contributions to the capture cross section. Column 6 shows the assumed energy dependence for the level spacing. The p-wave strength function obtained has an average value of about $2.0 \times 10^{-4} \text{ eV}^{-1/2}$ with fluctuations of up to 15%.

The average parameters for s- and p-waves used in the fitting as indicated above plus the fitted S_1 of Table 6 are included as unresolved parameters in File 2 of the ENDF/B data. The d-wave contribution was included as a pointwise tabulated cross section in File 3 of the data.

G. Capture Cross Section and Missed Levels

Since many p-wave resonances and perhaps a few s-wave resonances below 3.9 keV have not been resolved, it is necessary to estimate the capture

Table 6. Components of Capture Cross Section and Fitted p-wave Strength Function						
Energy keV	σ_γ s-wave	σ_γ p-wave	σ_γ d-wave	Net* σ_γ	$\langle D_0 \rangle$	Fitted $S_1 \times 10^4$
3.91	.7074	.4026		1.110	20.80	1.950
4.5	.6255	.3985		1.025	20.78	1.866
5.5	.5245	.3155		0.940	20.75	1.880
6.5	.4525	.4375		0.890	20.71	1.965
7.5	.3987	.4343		0.833	20.67	1.938
8.5	.3569	.4331		0.790	20.63	1.920
9.5	.3234	.4326	.002	0.759	20.59	1.933
12.0	.2629	.4371	.005	0.705	20.51	2.046
15.0	.2158	.4272	.007	0.650	20.39	2.153
20.0	.1673	.3827	.010	0.560	20.19	2.034
25.0	.1375	.3465	.014	0.498	20.00	1.962
30.0	.1170	.3210	.018	0.456	19.83	1.947
35.0	.1021	.2979	.023	0.423	19.66	1.934
40.0	.0909	.2821	.027	0.400	19.49	2.016
45.0	.0821	.2639	.032	0.378	19.33	1.981

* Evaluated capture cross section (see section III-B) used to obtain fitted S_1 .

cross section contribution from the missed levels. Based on average level spacing considerations, it appears reasonable for the background cross section estimation, to assume that all s-wave resonances up to 3.91 keV and all p-wave resonances up to 600 eV have been resolved. The background capture cross section was then estimated as approximately the difference between the p-wave cross section obtained from a statistical calculation ($D = 20.8$ eV, $S_0 = 0.9 \times 10^{-4}$, $S_1 = 2.0 \times 10^{-4}$, and $\Gamma_\gamma = 23.5$ MeV) and that calculated from the resolved p-wave parameters. Table 7 gives the contributions to the net σ_γ (column 6 of Table 7) along with the results of the statistical calculations and the measure-

Table 7. Contributions to (n, γ) Cross Section in Resolved Energy Range

Resolved Resonances						Statistical Calculation			
ΔE keV	s-wave 188 Res.	p-wave 62 Res.*	p-wave 148 Res.	Background Estimation	Net σ_γ	s-wave	p-wave	Total σ_γ	σ_γ Measurements of Moxon [19]†
0.0-0.1	45.65	0.008	0.019	0.0	45.68				
0.1-0.2	16.35	0.015	0.027	0.0	16.39	10.5	0.101	10.60	
0.2-0.3	8.05	0.156	0.060	0.0	8.27	7.08	0.130	7.21	
0.3-0.4	2.52	0.036	0.056	0.0	2.61	5.41	0.153	5.56	
0.4-0.5	2.17	0.109	0.064	0.0	2.34	4.41	0.173	4.58	
0.5-0.6	4.47	0.074	0.057	0.0	4.60	3.73	0.191	3.92	3.85 \pm .13
0.6-0.7	3.02	0.112	0.075	0.017	3.22	3.25	0.206	3.46	3.00 \pm .11
0.7-0.8	1.39	0.082	0.077	0.065	1.61	2.89	0.221	3.11	1.71 \pm .08
0.8-0.9	2.64	0.084	0.070	0.090	2.88	2.60	0.234	2.83	2.78 \pm .10
0.9-1.0	3.68	0.062	0.085	0.092	3.92	2.37	0.246	2.62	3.12 \pm .11
1.0-2.0	1.55	0.087	0.078	0.138	1.85	1.61	0.275	1.89	1.77 \pm .08
2.0-3.0	1.01	0.028	0.007	0.320	1.37	1.04	0.360	1.40	1.37 \pm .07
3.0-3.9	0.83	0.015	0.0	0.380	1.23	0.773	0.397	1.17	1.16 \pm .06

* Approximately the 62 largest p-wave reduced neutron widths.

† A normalization of 1.09 not given in this column, was applied to Moxon data in this evaluation. See Section III-B.

ments of Moxon [19]. Agreement of the net σ_γ with the Moxon data is about 5% except for the intervals 0.5 - 0.6 and 0.9 - 1.0 keV where the Moxon data are lower by 20 - 25%. Both of these intervals have large resonances within 10 eV of the top of the interval so that resolution differences could be significant in the Moxon data comparisons for these intervals. Current processing codes for ENDF/B data tend to be limited to 250 resolved resonances. Inclusion of all 214 p-wave resonances in Table 3 would also require excessive computer time for processing the data into multigroup constants for reactor calculations. For these reasons, only 62 of the largest p-wave resonances (as indicated by + in Table 3) were included with the 188 s-wave resonances as resonance parameters in File 2 of the ENDF/B data. Five resonances (as indicated by * in Table 2) were dropped from the evaluation as they have a negligible contribution to σ_γ and would require excessive energy points to describe by pointwise data. The other 147 resonances in Table 3 were included as File 3 pointwise cross sections based on calculations using the parameters of Table 3.

III. TABULATED POINTWISE CROSS SECTION DATA

This chapter describes the evaluations for: all cross sections below 5.0 eV, capture, fission, $\bar{\nu}$, (n,2n), (n,3n), total, nonelastic and elastic scattering cross sections. Evaluation of the inelastic scattering cross sections is given in Chapter IV. Angular distributions for elastic scattering were not reevaluated in the present effort and the previous ENDF/B evaluation [1] was retained for the distributions.

A. Cross Sections Below 5.0 eV

Cross sections from 10^{-5} to 5.0 eV were obtained from an evaluation by Leonard [15] conducted concurrently with the present evaluation above 5.0 eV. The 0.0253 eV capture cross section is 2.72 b., based primarily on the measurement of Bigham [16]. The shape of the cross sections is deduced from the positive energy levels of the current evaluation, four negative levels including one with parameters determined by the simultaneous requirement of the normalization value of 2.72 b., a fit to

the total cross section data of Bollinger [17] in the region 1 - 5 eV, and a potential scattering cross section of 10.6 b. Resonance parameters for the 6.67 eV resonance which strongly influences the thermal cross sections are $\Gamma_n = 1.50$ MeV and $\Gamma_\gamma = 25.6$ MeV.

B. Capture Cross Section

In Version II of the ENDF/B file, emphasis has been placed on consistent normalization of the experimental data with ^{235}U fission from the evaluation of Davey [18] adopted as the primary standard cross section. In addition, the $^{10}\text{B}(n,\alpha)$ cross section, as utilized by Moxon [19], has been used for normalization in this evaluation. Davey [20] has reported a ^{238}U capture evaluation emphasizing ^{235}U fission normalization. The selection of reliable experimental data in the present evaluation follows closely that of Davey [20] although differing somewhat in final data adjustments.

Above 100 keV, the majority of accurate capture measurements are relative to ^{235}U fission, such as Barry [21] and Poenitz [22,23], while the Menlove and Poenitz [24] data can be placed relative to ^{235}U fission by use of the fission cross section of Poenitz [25] obtained by the same experimental techniques. These four sets of data were normalized to the ENDF/B [18,26] ^{235}U fission cross section and are shown in Figure 1. In general, the data are in agreement within experimental errors ($\sim 5\%$) between 0.2 and 1.0 MeV. The discrepancy of up to 15% between Barry [21] and Poenitz [23] above 1.0 MeV is significant as it could extend beyond 1.5 MeV where the only reliable data is that of Barry. The discrepancy of 10 - 15% between 0.12 and 0.16 MeV is particularly notable in that the lower limit of the data at these energies is required for consistent extrapolation to the capture data below 100 keV (Moxon [19]) measured relative to $^{10}\text{B}(n,\alpha)$.

The evaluated capture cross section above 100 keV is based on the well-agreeing ratio data. Figure 2 compares the evaluated ratio of ^{238}U capture to ^{235}U fission with experimental data and the evaluation of Davey [20].

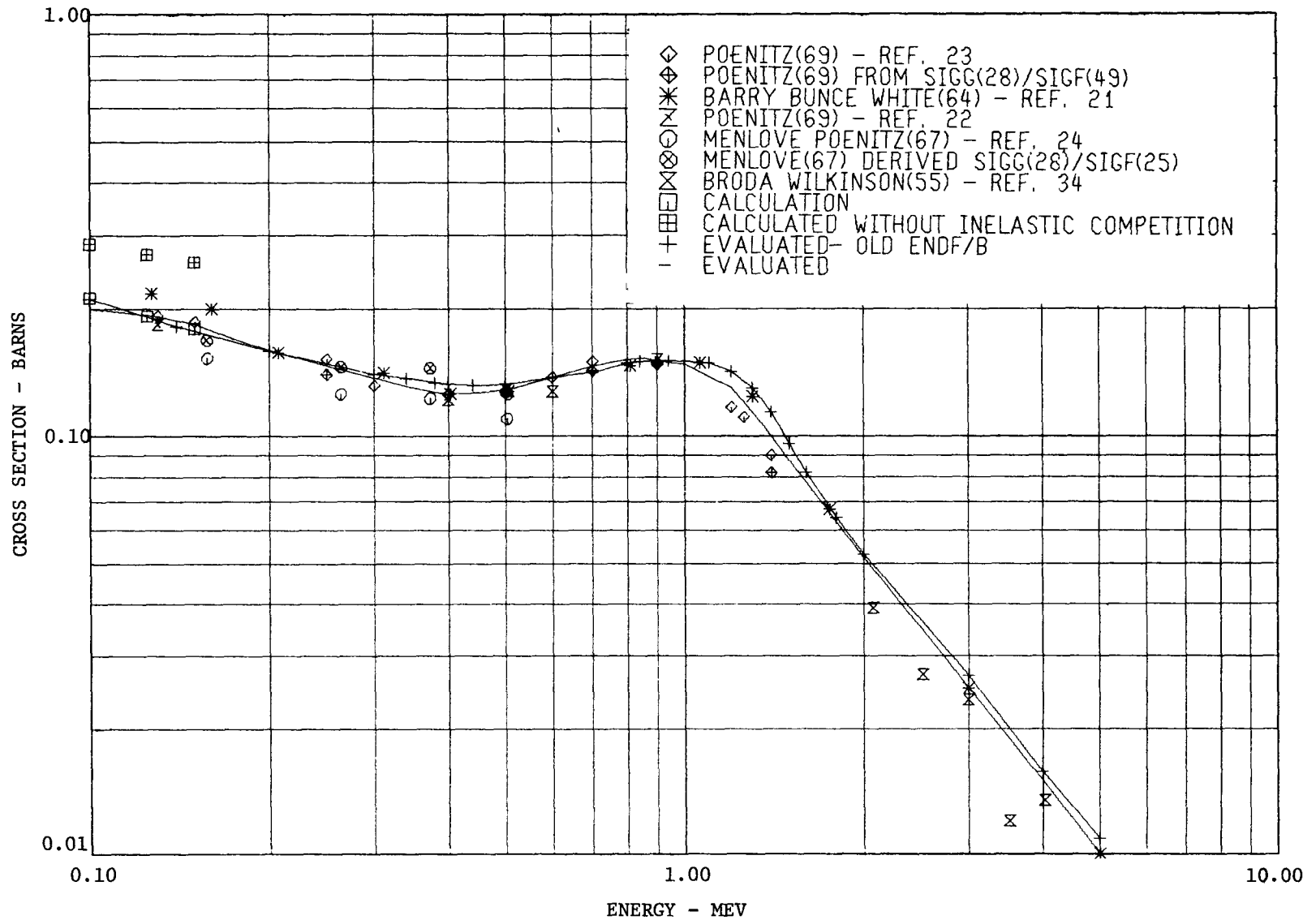


Figure 1. Comparison of Experimental and Evaluated Capture Cross Sections Between 0.1 and 10 MeV

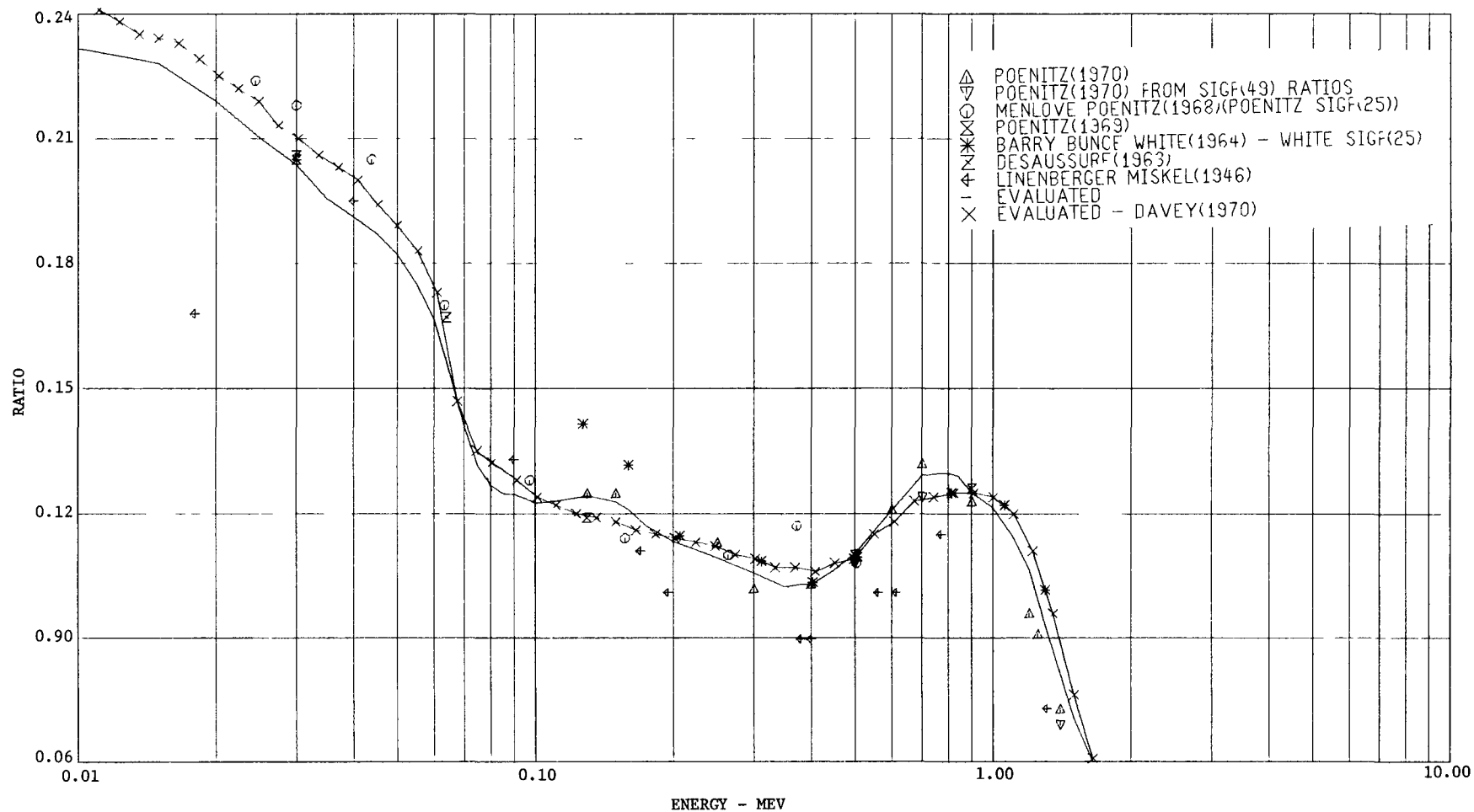


Figure 2. Comparison of Experimental and Evaluated Ratios of ^{238}U Capture/ ^{235}U Fission

Below 100 keV, the experimental data on ^{238}U capture is highly discrepant as shown in Figure 3. The most accurate shape measurement of the cross section is that of Moxon [19] between 0.5 and 100.0 keV. This measurement, relative to $^{10}\text{B}(n,\alpha)$, is also one of the most accurate measurements with a quoted accuracy of 3 - 6%. Other measurements of significant accuracy ($\lesssim 10\%$) are those given in Table 8 at 30 keV with additional measurements by de Saussure [27] and Gibbons [28] at 64 keV and Menlove [24] at 24.4, 43.8, 63.3, and 97.3 keV. The latter measurements can at least be traced to ^{235}U fission normalization and tend to be 10 - 15% higher than the Moxon [19] data which alone supports very low capture cross sections. Similarly the Moxon data at 100 keV is lower than the evaluated cross section above 100 keV for which the ^{238}U capture/ ^{235}U fission ratio appears to be well established. Unfortunately, accurate ^{235}U fission/ $^{10}\text{B}(n,\alpha)$ measurements, which could help to resolve the present discrepancies, are not available.

The relatively large number of 30 keV measurements permit a "best estimate" for further normalizations of the data. The most reliable 30 keV measurements, given in Table 8, were averaged to obtain 0.456 b. for the 30 keV cross section. Data offering significant shape information, of which the Moxon data are clearly the most accurate, were normalized to 0.456 b. at 30 keV. For the Moxon data, the normalization factor is 1.09 and the evaluated curve is based primarily on the normalized Moxon data from 3.9 to 100.0 keV as shown in Figure 3.

The Moxon data shows a drop in the cross section above 50 keV most likely resulting from inelastic scattering competition from the 45 keV level. This drop in the cross section was examined by statistical calculations using the average parameters given in Section II-F plus inelastic widths estimated by assuming the inelastic strength function for each open channel to be the same as the corresponding p- and d-wave strength functions for elastic scattering. Chi-squared distributions for the inelastic widths were assigned assuming that the number of degrees of freedom (ν values) is equal to the number of open channels. Penetration factors for the inelastic widths were also obtained similarly to elastic widths but were calculated using the excess energy above the inelastic

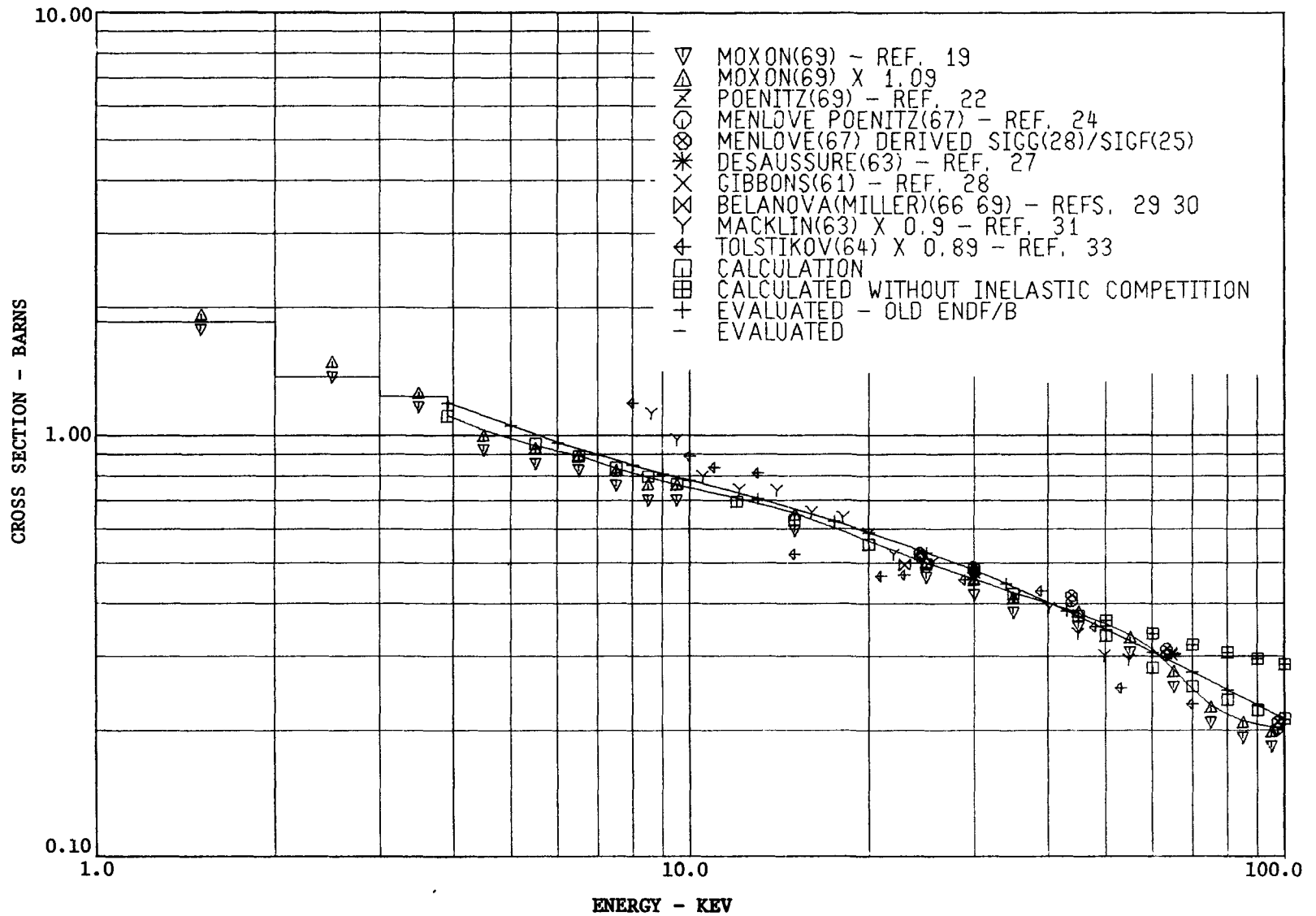


Figure 3. Comparison of Experimental and Evaluated Capture Cross Sections Between 1 and 100 keV

Table 8. Summary of 30 keV (n, γ) Data Used in Evaluation

Experiment	Type and Value of Measurement	Adjusted σ_{γ}^*
Poenitz (1969)[22]	$\sigma_{\gamma}^{28}/\sigma_f^{25} = .205 \pm .008$	$0.459 \pm .022$
de Saussure (1963)[27]	$\sigma_{\gamma}^{28}/\sigma_a^{25} = .150 \pm .012$	$0.461 \pm .040$
Gibbons, et. al. (1961)[28]	$\sigma_{\gamma}^{28} = .473 \pm .05$ relative In = .763	$0.473 \pm .06$
Menlove (1968)[24]	Absolute $.473 \pm .015$	$0.473 \pm .02$
Belanova (Miller)(1966, 1968)[29, 30]	Absolute $\sigma_{\gamma}^{28}(23 \text{ keV}) = .495 \pm .04, \frac{\sigma_{\gamma}(30)}{\sigma_{\gamma}(23)} = .91$	$0.450 \pm .04$
Macklin (1963)[31]	Relative Ta - Davey [12] = $.507 \pm .051$	$0.507 \pm .08$
Moxon, Chaffee (1966)[32]	Relative B ¹⁰ (n, α), $\sigma_{\gamma}^{28} = .403 \pm .062$	$0.403 \pm .062$
Moxon (1969)[19]	Relative B ¹⁰ (n, α), $\sigma_{\gamma}^{28} = .418 \pm .029$	$0.418 \pm .029$
Average	Reciprocal Weighting by (uncertainty) ²	0.456

*Normalization Values

$\sigma_f^{25} = 2.24 \pm .05$

$\alpha^{25} = .372 \pm .03$

$\sigma_{n,\alpha}^{B10} = 3.41 \pm .07$

threshold. Results of the calculations both with and without inelastic scattering are shown in Figures 1 and 3. The statistical calculations confirm the magnitude of the drop in the cross section found by Moxon above 45 keV although the relatively simple calculational model differs somewhat in the shape of the cross section.

C. Fission Cross Section

The most accurate ^{238}U fission data have been measured as $^{238}\text{U}/^{235}\text{U}$ fission ratios by Lamphere [35], Stein [36], and White and Warner [37]. Measurements by Smith [38] of absolute ^{238}U and ^{235}U fission cross sections have recently been revised by Hansen [39] on the basis of calculated scattering corrections to the original measurements. Fission ratios obtained from the Hansen data are shown with other ratio data in Figure 4. The original Lamphere data [35] have been decreased by 6% following the recommendation of Davey [18], based on normalization to the more accurate ($\pm 1\%$) measurements of Stein [36] at 1.5, 2.0, 2.5, and 3.0 MeV. In the overlapping energy range between 2.0 and 5.0 MeV, the ratios obtained from the Hansen data are in excellent agreement with the data of Stein. At 5.4 and 14.1 MeV, discrepancies between White [37] and Hansen are 5% and 3% respectively.

The fission ratio data were evaluated to obtain the curve given in Figure 4. Accuracy of the evaluated fission ratio is about 5% below 2 MeV, 2% between 2 and 5 MeV, and 5% between 5 and 15 MeV. The evaluated fission ratio was combined with the ENDF/B ^{235}U fission cross section [18,26] to obtain the ^{238}U fission cross section. Other ^{238}U fission measurements such as Kalinin and Pankratov [40] or the shape measurements of Henkel [41] and Pankratov [42] are not sufficiently accurate to resolve remaining discrepancies in the fission cross section.

An average of the evaluated fission cross section over the Watt spectrum for thermal ^{235}U fission yields 0.284 b., which is about 8% lower than experimental values of 0.304 ± 0.007 [43], 0.310 ± 0.004 [44], and 0.31 ± 0.01 [45]. The 14 MeV cross section in the present evaluation is 1.075 b. compared to an average value of 1.13 b., indicated

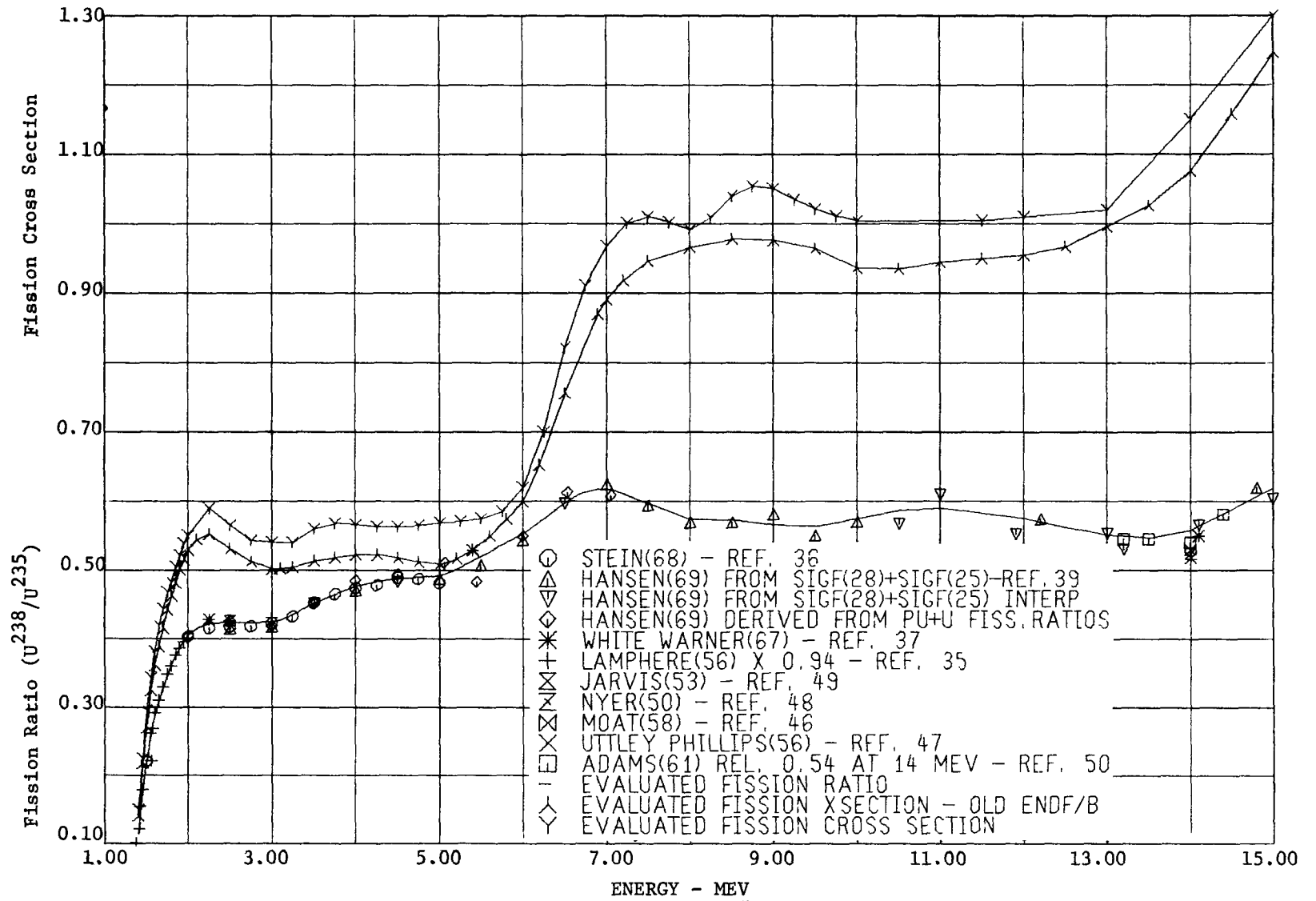


Figure 4. Comparison of Experimental and Evaluated Fission Ratio and of Evaluated Fission Cross Sections

by absolute measurements [46,47,48]. These comparisons, as well as numerous integral experiment analyses which yielded good agreement between calculation and experiment with about 5 - 10% higher fission cross sections than the present evaluation, tend to indicate that the presently evaluated fission cross section may be too low by 5 - 8%. A discrepancy of this size appears to be outside the range of uncertainty in the $^{238}\text{U}/^{235}\text{U}$ fission ratio and is likely, at least in part, due to an underestimation of the ^{235}U fission cross section, particularly above 2.5 MeV where the Hansen data [39] was used for the ENDF/B ^{235}U evaluation.

The recommended ^{238}U fission spectrum is a Maxwellian distribution based on the formula of Terrell [80] for the nuclear temperature using the evaluated value of neutrons per fission, $\bar{\nu}$. The temperature is given as a linear interpolation between a temperature of 1.31 MeV at 1.0 MeV neutron energy and 1.53 MeV at 15.0 MeV based on an evaluation by Drake [56].

D. Average Number of Neutrons per Fission - $\bar{\nu}$

The average number of total neutrons per fission is given by $\bar{\nu} = 2.337 + 0.1521E(\text{MeV})$ based on an evaluation by Drake [56] which included the recent measurements of Soleilhac [57]. Normalization for $\bar{\nu}$ is based on the 1969 evaluation of Hanna [58].

E. (n,2n) Cross Section

The original measurements of the (n,2n) cross section by Knight [51] and Graves [52] have been corrected by Barr [53] leading to adjustments of up to +10% to the data of Knight and up to $\pm 10\%$ to the data of Graves. These data represent the only measurements on (n,2n) except for measurements near 14 MeV by Mather [54] and Barr [53]. However, the normalization of the data as corrected by Barr is not known. In addition, there is some question on normalization of the original Knight [51] data as the data are reported as ratios relative to an "apparent" ^{238}U fission cross section which is uncorrected for the low energy neutrons from the $\text{D}(d,np)\text{D}$ reaction used in the experiments.

Since the Knight and Graves data as published were normalized using fission data from the measurements of Smith, Henkel and Nobles [38], it is assumed for this evaluation that the data as corrected by Barr are also consistent with this normalization. Ratios of (n,2n)/fission were then obtained using the Barr corrections to the Knight and Graves data together with the ^{238}U fission cross sections of Smith, Henkel and Nobles. These ratios were then combined with the present evaluation for ^{238}U fission to obtain the Knight and Graves data used in this evaluation.

The evaluated and experimental data for the (n,2n) cross section are shown in Figure 5.

The secondary energy distribution from the (n,2n) reaction has not been measured. For this evaluation, it is assumed that the secondary distribution can be described as Maxwellian. The work of Le Couteur [55] indicates that a reasonable approximation for the average energy of the emitted particles is

$$\bar{E} = 2T = \frac{4T_0}{3}$$

where T_0 is the temperature of the first emitted neutron. For neutron energies such that the excess energy above the (n,2n) threshold is greater than the average energy obtained from this expression, $T = 2T_0/3$ was used for the (n,2n) temperature where T_0 is the inelastic scattering temperature (see section IV-D). The excess neutron energy above the threshold is less than $4T_0/3$ below about 8 MeV. In the energy range between threshold and 8 MeV, it is assumed that the two neutrons share 80% of the available energy. Then

$$\bar{E} = 2T = \frac{0.8(E_n - 6.07)}{2}$$

$$T = 0.2(E_n - 6.07)$$

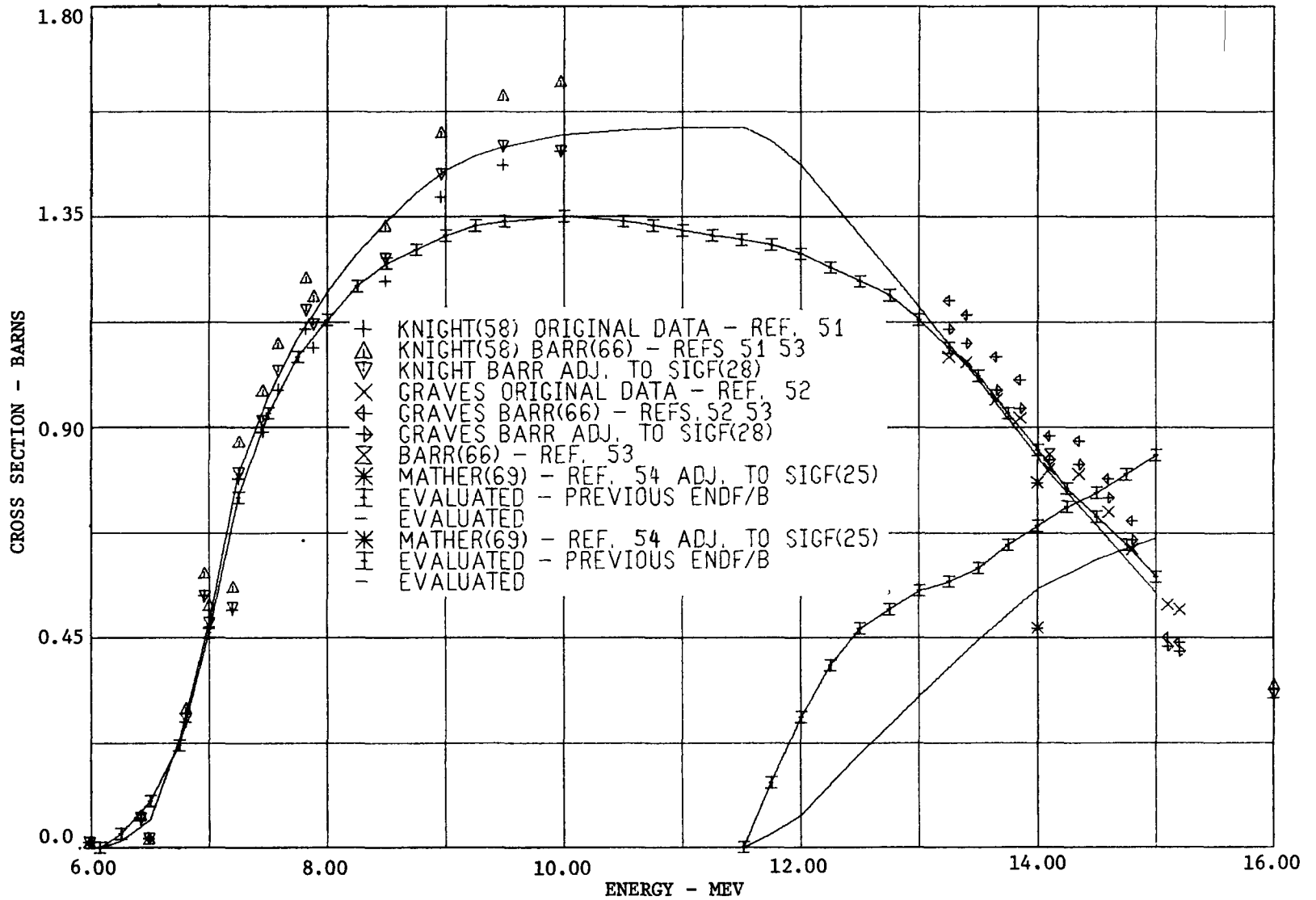


Figure 5. Comparison of Experimental and Evaluated (n,2n) and (n,3n) Cross Sections

This expression for the (n,2n) temperature was joined smoothly with $T = 2T_0/3$ near 8 MeV to define the (n,2n) temperature.

F. (n,3n) Cross Section

The only reported (n,3n) cross section measurement with significant accuracy is the 14 MeV value of Mather [54]. The present evaluation is based on this measurement and is shown in Figure 5.

For the (n,3n) reaction, the secondary energy distribution is assumed to be Maxwellian with a temperature estimated by interpolating from approximately 0 at the threshold energy to a 15 MeV value of 2/3 the (n,2n) temperature plus 1/3 the inelastic scattering temperature evaluated at

$$E = 0.8(15 - 11.51 - 2 \bar{E}_{n,2n})$$

where 11.51 MeV is the (n,3n) threshold energy.

G. Total Cross Section

Experimental and evaluated data for the total cross section are shown in Figures 6 and 7. In these figures, the detailed pointwise data of Whalen [60] have been averaged over 20 keV intervals below 700 keV and 30 keV intervals above 700 keV. Similarly, the data of Foster [61] in the figures have been averaged over energy intervals.

The evaluated cross section is based primarily on the data of Whalen [60] and Uttley [59] below 0.7 MeV, Whalen [60] between 0.7 and 1.5 MeV, Henkel [62] and Uttley [59] between 1.5 and 2.2 MeV and Foster [61] and Uttley [59] above 2.2 MeV.

H. Nonelastic Cross Section

The nonelastic cross section up to 2.00 MeV was obtained as a summation of the capture, fission and inelastic scattering cross sections. Experi-

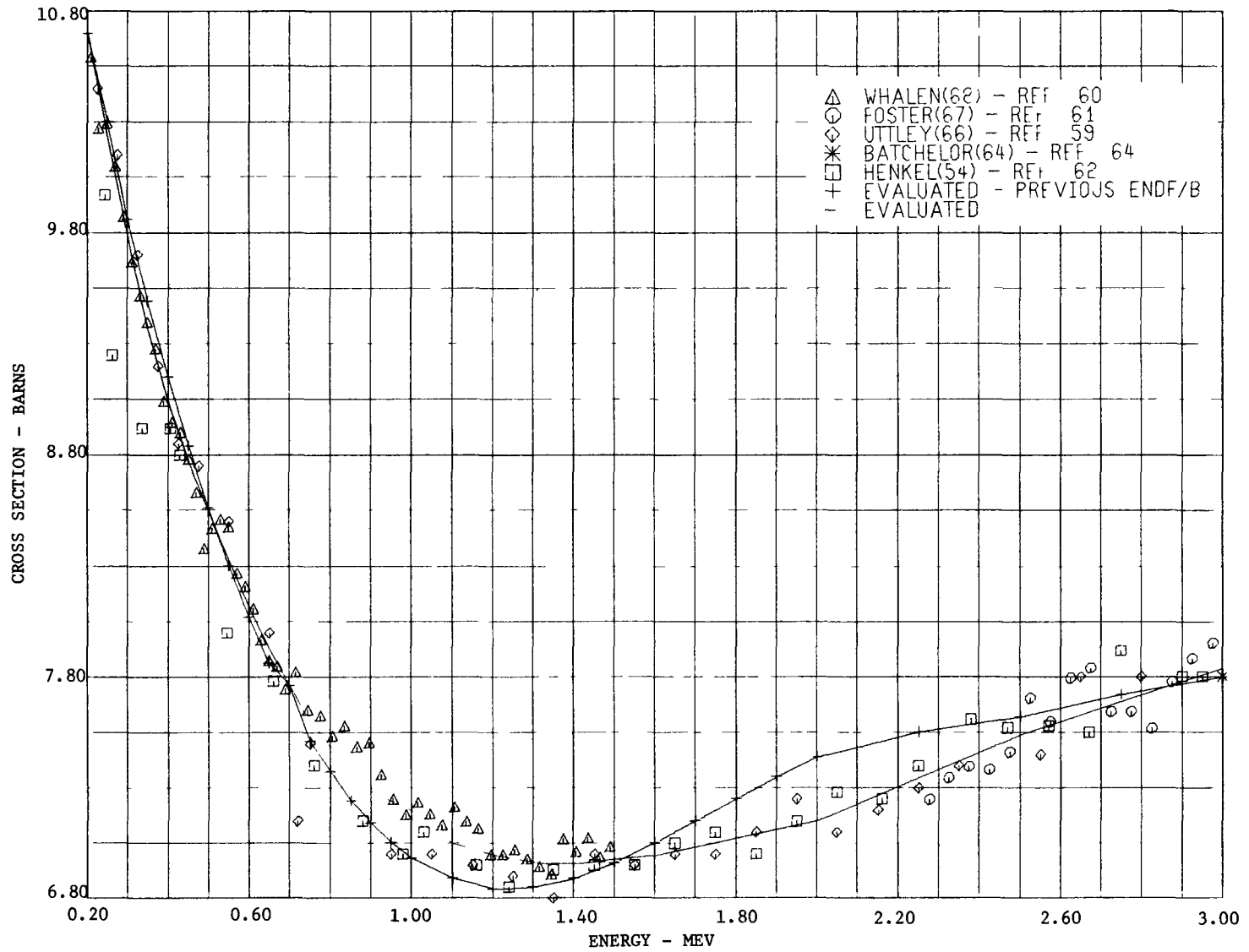


Figure 6. Comparison of Experimental and Evaluated Total Cross Sections--0.2 to 3.0 MeV

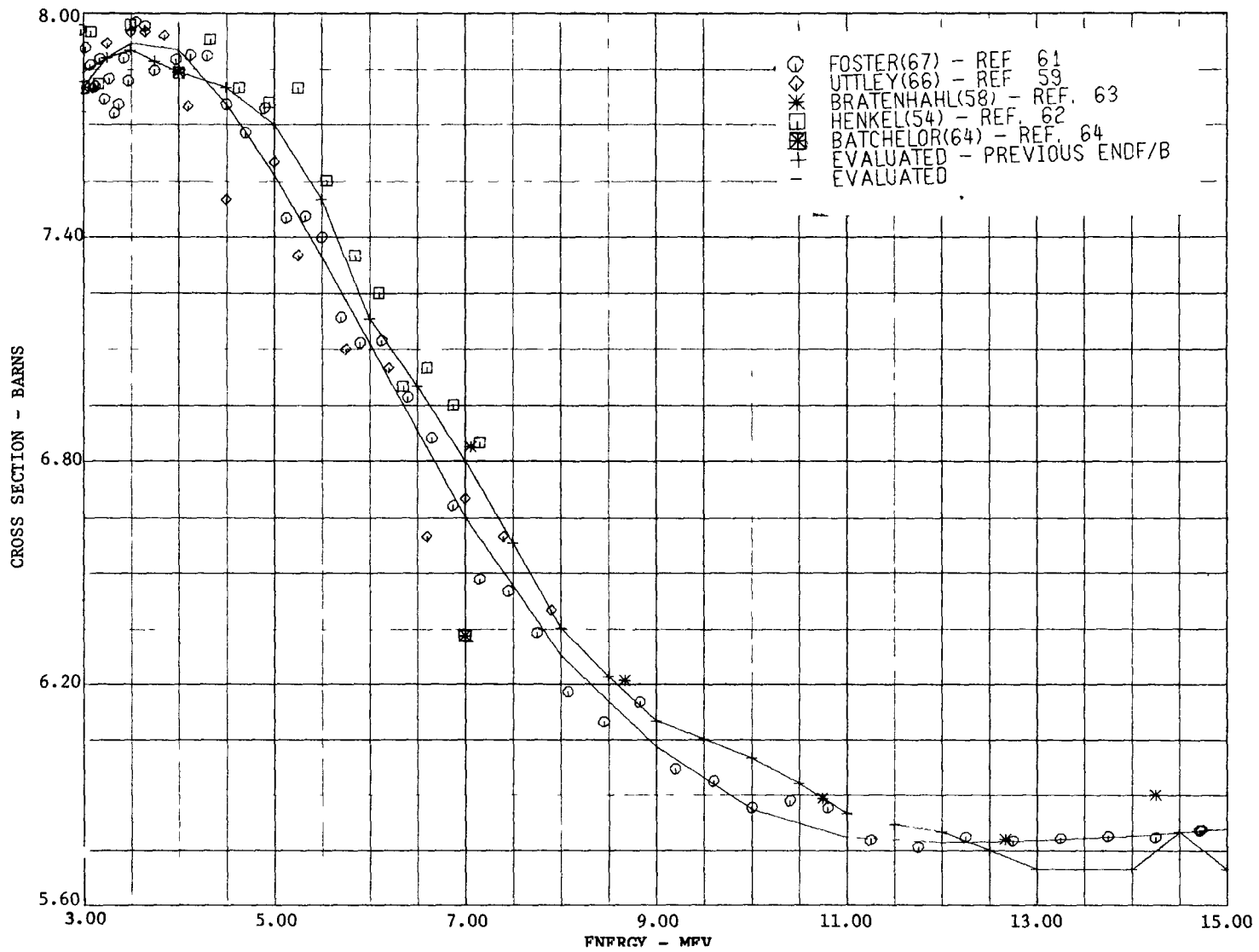


Figure 7. Comparison of Experimental and Evaluated Total Cross Sections--3.0 to 15.0 MeV

mental and evaluated data for the nonelastic cross section above 2.0 MeV are shown in Figure 8. The experimental data in this figure include inelastic scattering only to levels above about 0.6 MeV as levels below this energy have not been separable from elastic scattering in the measurements. The value of 3.08 b. at 2.0 MeV assigned to Batchelor [64] in Figure 8 was obtained as the difference between Batchelor's 2.0 MeV elastic scattering measurement of 4.07 ± 0.2 b. and the evaluated total cross section of 7.15 b.

The present evaluation is in good agreement above 2.5 MeV with the previous ENDF/B evaluation [1] and the evaluation of Schmidt [72] with maximum deviations of about 3%.

I. Elastic Scattering Cross Section

The elastic scattering cross section was obtained as the difference between the evaluated total and nonelastic cross sections. Figure 9 compares evaluated and selected experimental data for elastic scattering. Difficulties in comparison with experiment arise due to the lack of separation of elastic scattering from low energy level inelastic scattering. The data of Smith [73] in Figure 9 is shown as reported by Smith including inelastic scattering and as corrected for inelastic scattering. Below 1.17 MeV, Smith was able to experimentally separate elastic scattering from inelastic scattering for all levels. Above this energy, the measured data included the 45 keV level and sometimes the 145 keV level and Smith corrected his data for these levels as shown in Figure 9. All experimental data above 2.0 MeV include at least the first two levels from inelastic scattering. The data from this evaluation in Figure 9 are shown as the evaluated elastic plus the alternate curves including one or two inelastic levels.

IV. INELASTIC SCATTERING CROSS SECTIONS

Recent measurements of the ^{238}U inelastic scattering cross section by Smith [74] provide a check against the extensive measurements of Barnard [75] and Smith [73] as well as the measurements by Cranberg [76] and

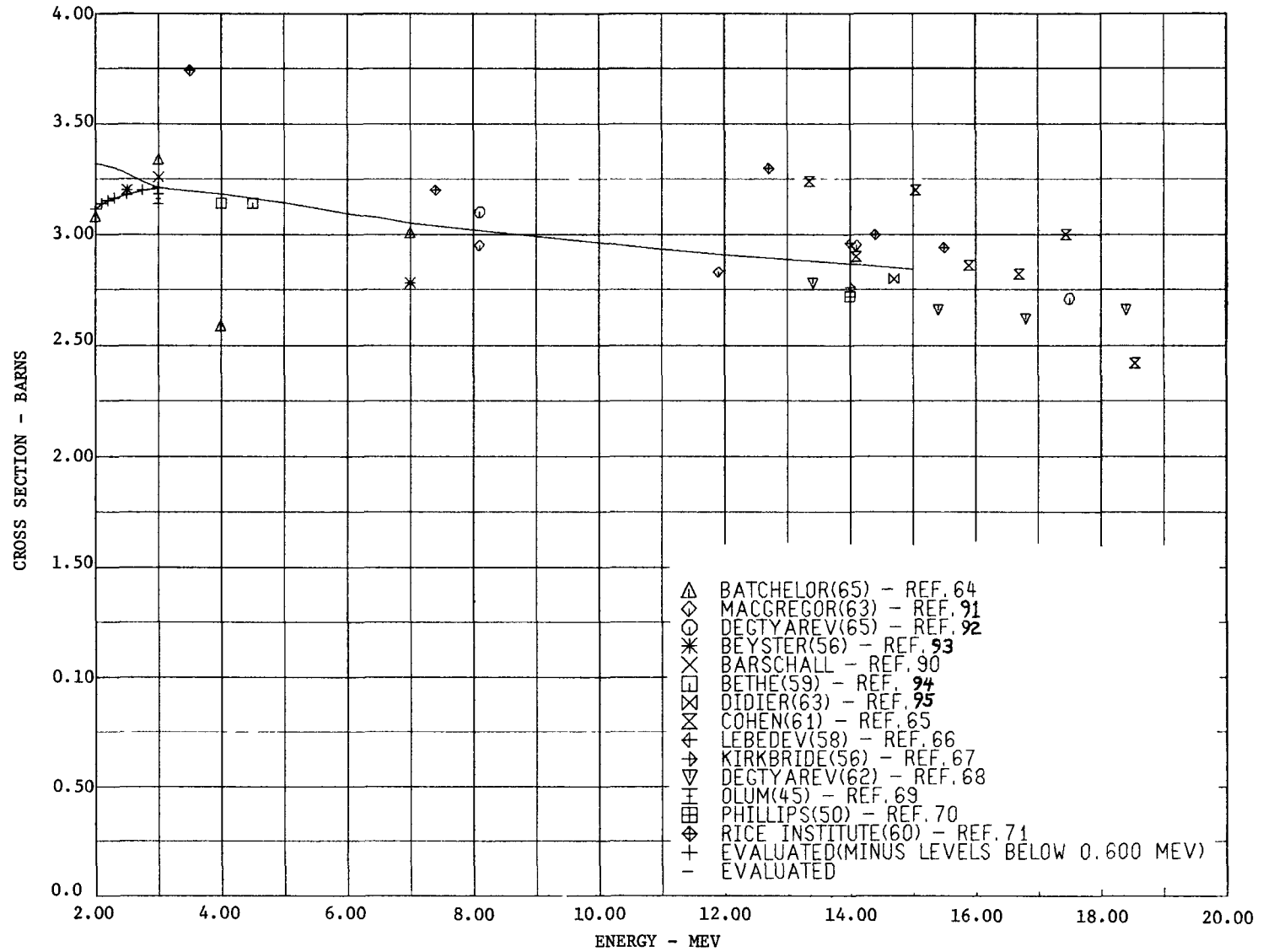


Figure 8. Comparison of Experimental and Evaluated Non-elastic Cross Sections

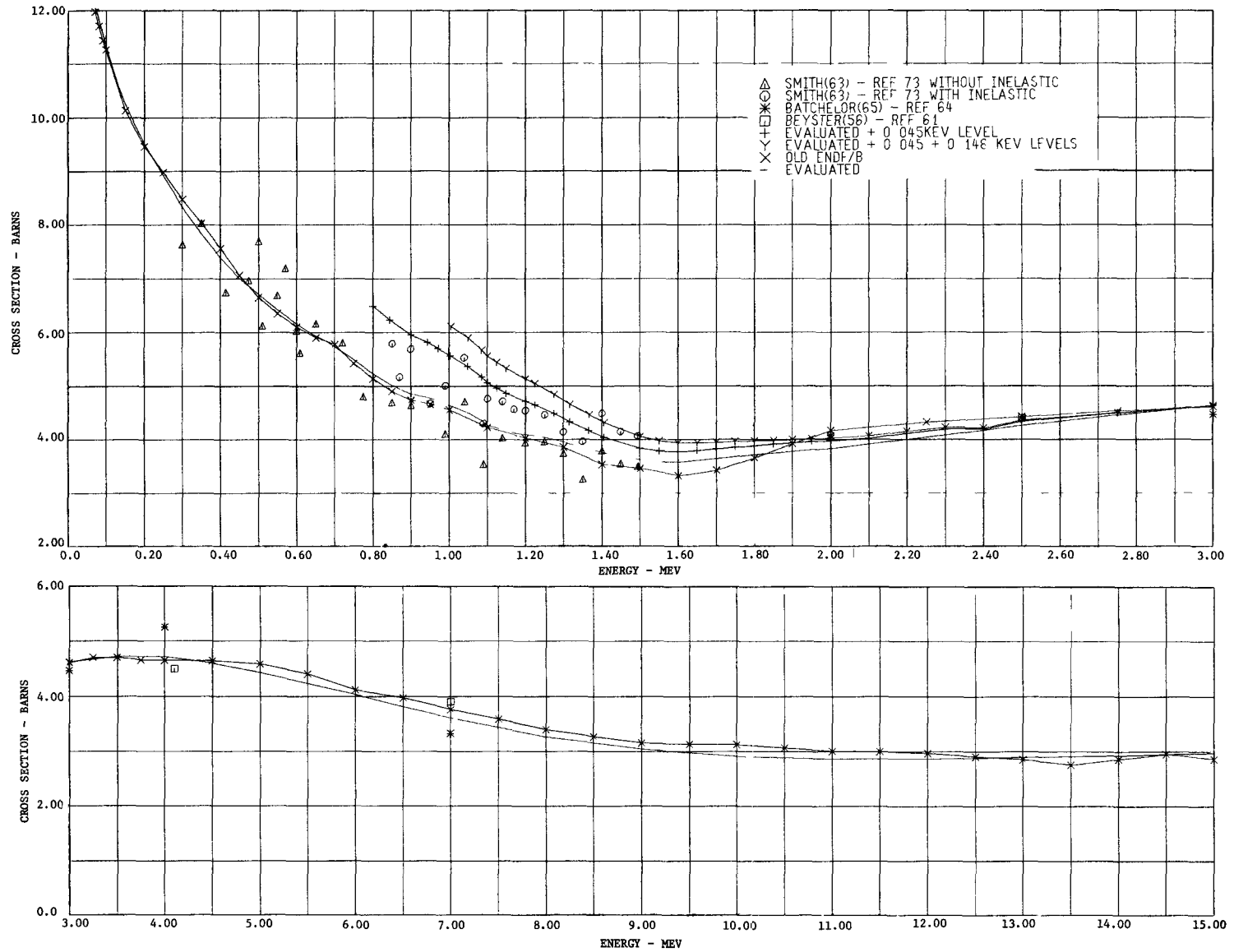


Figure 9. Comparison of Experimental and Evaluated Elastic Scattering Cross Sections

and Glazkov [77]. The new measurements of Smith [74] permit a reassessment of the inelastic scattering cross section of the Version I ENDF/B data [1] which is based on the evaluation of Schmidt [72]. The resolved level structure for the present evaluation, resolved level cross sections, statistical scattering cross section above the resolved levels and the secondary energy distribution for the statistical scattering are described in this section.

A. Level Structure

Smith [74] determined cross sections for 14 levels between 0.045 and 1.27 MeV with some measurements up to neutron energies of 1.69 MeV while Barnard reports cross sections for 22 levels between 0.045 and 1.47 MeV with measurements up to 1.62 MeV neutron energy. The level structure obtained in these two measurements is shown in Figure 10 along with the level structure used for the present evaluation. Up to 1.12 MeV, the levels found by Smith are essentially the same as those of Barnard. Smith reports a cross section only for a sum of the two levels at 0.939 and 0.968 found by Barnard while indicating that both levels exist.

Above 1.12 MeV, Smith could not isolate all the levels indicated by Barnard's data and the level correspondence between the two measurements is not uniquely defined. The level structure adopted for this evaluation above the 1.12 MeV level represents a compromise level structure for which the cross sections can be reliably defined from the combined data of Smith [74] and Barnard [75]. No attempt has been made to assess the validity of the more detailed level structure indicated by Barnard's results. The present evaluation then includes 19 resolved levels up to 1.45 MeV as indicated in Figure 10.

B. Resolved Levels

1. 0.0447 MeV Level

Measured data for the first level at 0.0447 MeV are shown in Figure 11. The data by Smith [73,74] represent integrations over measurements for

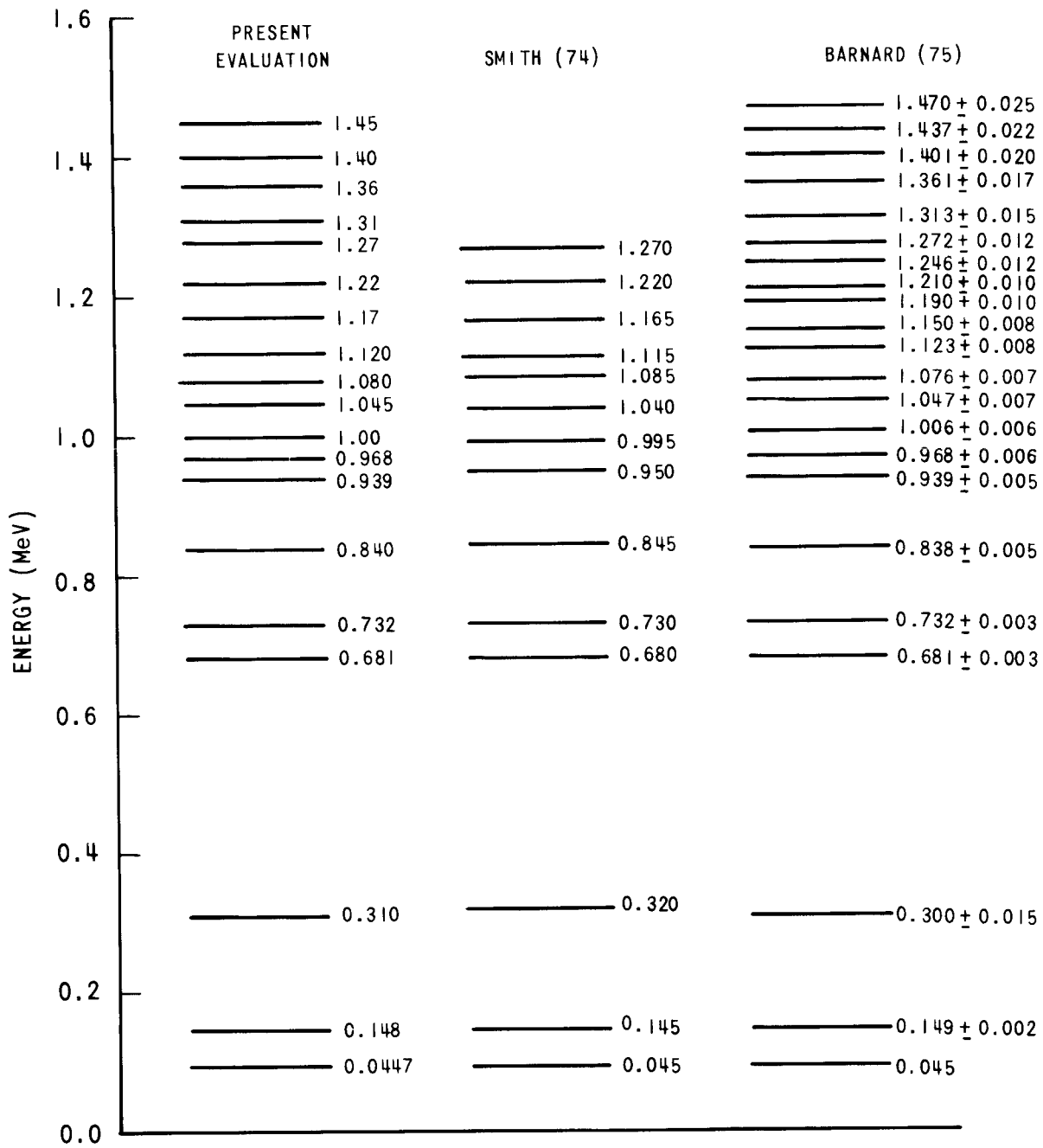


Figure 10. ^{238}U Level Structure for Inelastic Scattering

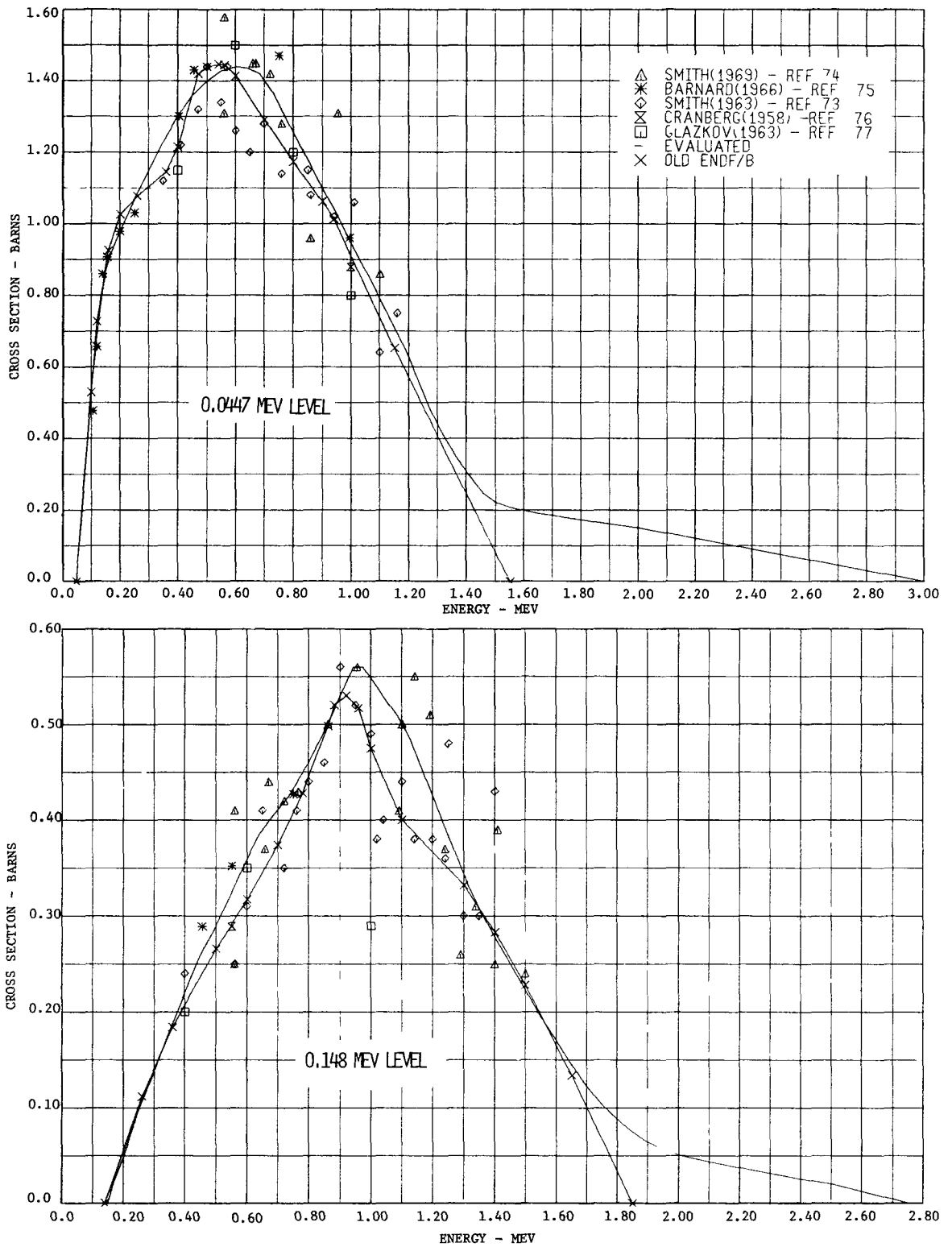


Figure 11. Inelastic Scattering Data for 0.0447 and 0.148 MeV Levels

a number of angles. Barnard [75] reports values measured at an angle of 90° and were multiplied by $0.95 \times 4\pi$ to obtain total inelastic cross sections. The factor of 0.95 is an estimated correction for angular asymmetry based on angular distributions reported by Smith [73]. The measurements of Smith [74] and Barnard [75] are in good agreement for this level and the evaluation is based primarily on these measurements up to 1.15 MeV.

Above 1.15 MeV, the cross section has not been measured and extrapolation of the cross section is somewhat arbitrary. Calculations by Dunford [78] and Prince [79] indicate that direct interaction contributions could lead to a cross section as large as 0.4 b. near 2.0 MeV and decreasing slowly above this energy. In general, measurements of elastic scattering and angular distributions above about 1.2 MeV have not been able to separate inelastic scattering from the 0.0447 MeV level (and frequently also the 0.148 MeV level) from elastic scattering. Assessment of a direct interaction cross section of the magnitude of 0.4 b. would require detailed comparisons with measured scattering angular distributions which have not been included in the present reevaluation of ENDF/B data. For reactor applications of the inelastic data, the separation of elastic and inelastic scattering for the 0.0447 MeV level above about 2.0 MeV is not particularly important provided that: the direct interaction contribution is assigned to level excitations rather than statistical secondary distributions and that angular distributions are appropriately separated for elastic and inelastic scattering. At this time, it is felt that large direct interaction contributions above 2.0 MeV are not sufficiently verified and the cross section was extrapolated to zero at 3.0 MeV.

2. 0.148 MeV Level

Measured data for the second level at 0.148 MeV are shown in Figure 11. For this level as well as all higher energy levels, the measurements of Barnard [75] have been multiplied by 4π (assumed to be isotropic) to obtain the total inelastic cross section for each level.

The recent measurements by Smith [74] indicate a larger cross section between 0.9 and 1.2 MeV than the earlier results of Smith [73]. The evaluated cross section is based on the 1970 results of Smith [74] up to 1.5 MeV and the Barnard data up to 1.0 MeV. Above 1.5 MeV, the cross section was smoothly extrapolated to zero at 2.5 MeV.

3. 0.310 MeV Level

Measurements for the 0.310 MeV level are shown in Figure 12. Recent measurements for this level by Smith [74] and Barnard [75] are notably discrepant from earlier results of Cranberg [76] and Glazkov [77]. The results of Smith indicate a much smaller cross section than Glazkov and form the basis for the present evaluation as shown in Figure 3.

4. 0.681 MeV Level

Data for the 0.680 MeV level are shown in Figure 12. The data of Smith [74] and Barnard [75] are in good agreement above 1.1 MeV although differing significantly near the peak of the cross section at 0.95 MeV. The present evaluation represents a compromise on the peak cross section at 0.95 MeV following through the well-agreeing data up to 1.6 MeV and extrapolated to zero at 2.5 MeV.

5. 0.732 and 0.838 MeV Levels

Figure 13 shows the experimental and evaluated data for the 0.732 and 0.838 MeV levels. In general, the experimental data are in good agreement for these levels and the evaluated curve is well defined below 1.5 MeV.

6. 0.939, 0.968 and 1.00 MeV Levels

Smith [74] obtained cross sections for a level at 0.945 MeV which represents the sum of the 0.939 and 0.968 MeV levels measured by Barnard [75]. A level found by Smith at 0.995 MeV corresponds to the 1.006 MeV level of Barnard. Figure 14 shows the data of Barnard for the 0.909 and 0.968 MeV levels, a comparison of the sum of Barnard's 0.939 and 0.968 MeV

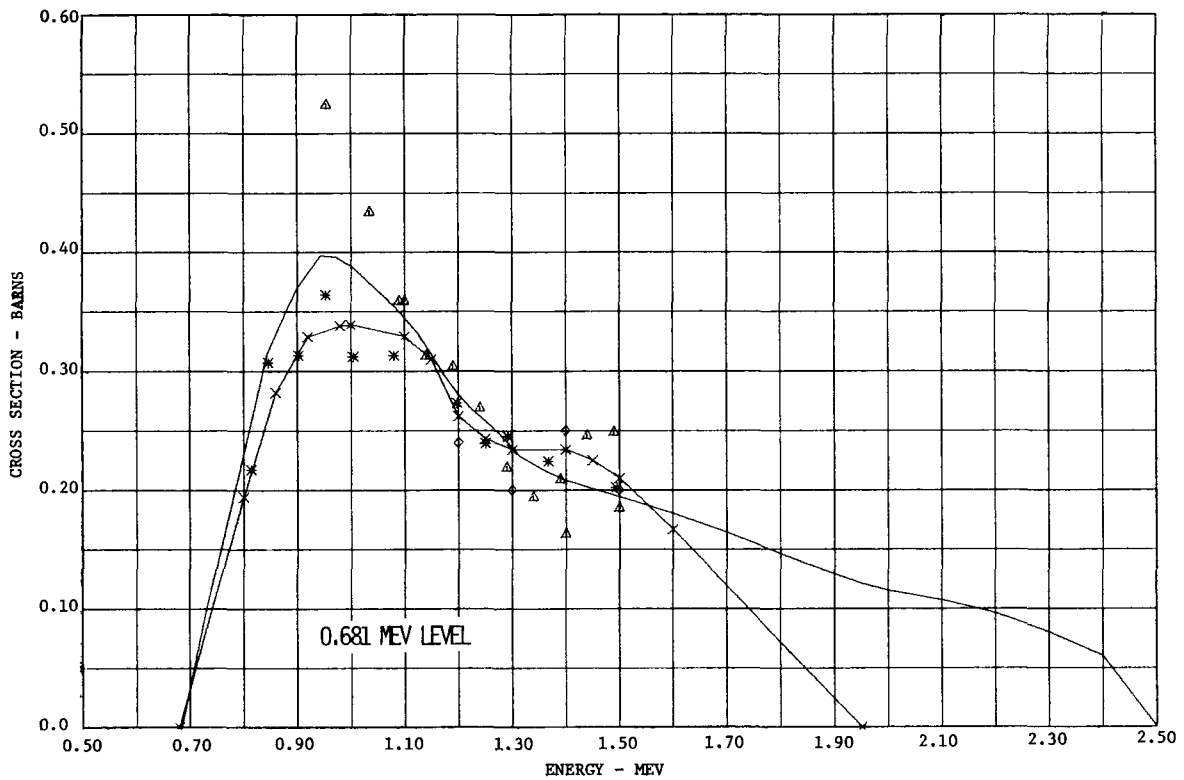
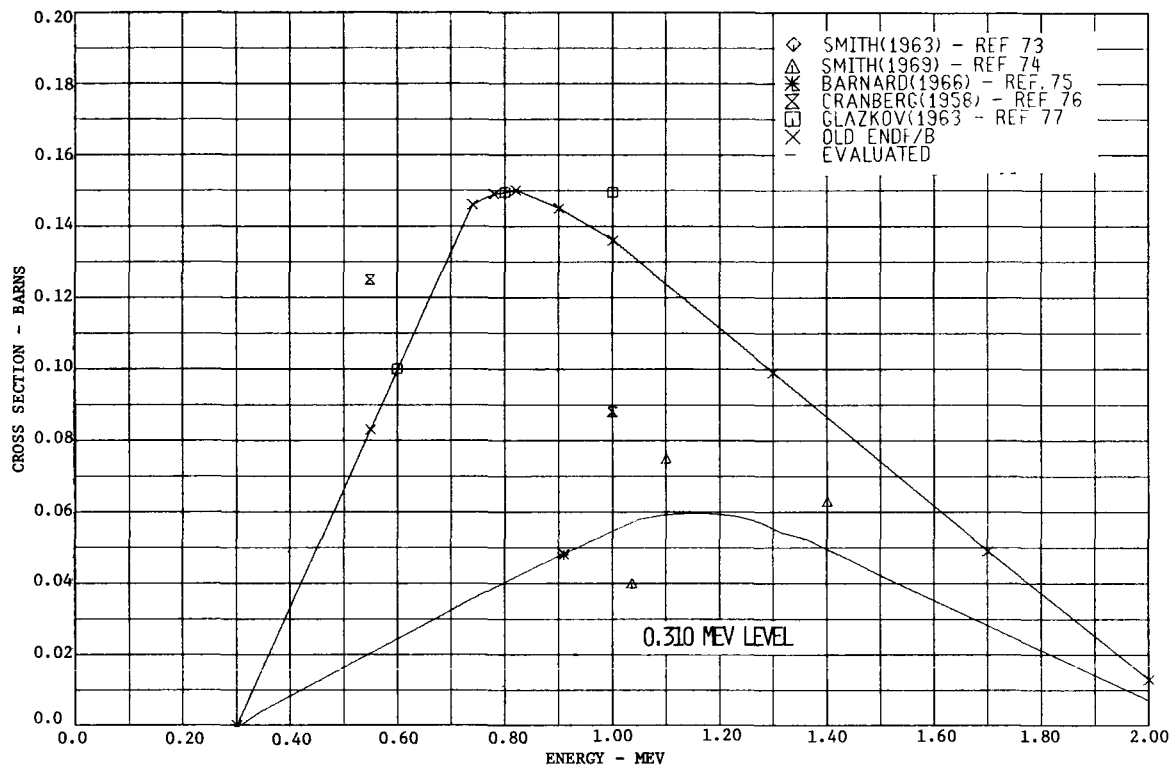


Figure 12. Inelastic Scattering Data for 0.310 and 0.681 MeV Levels

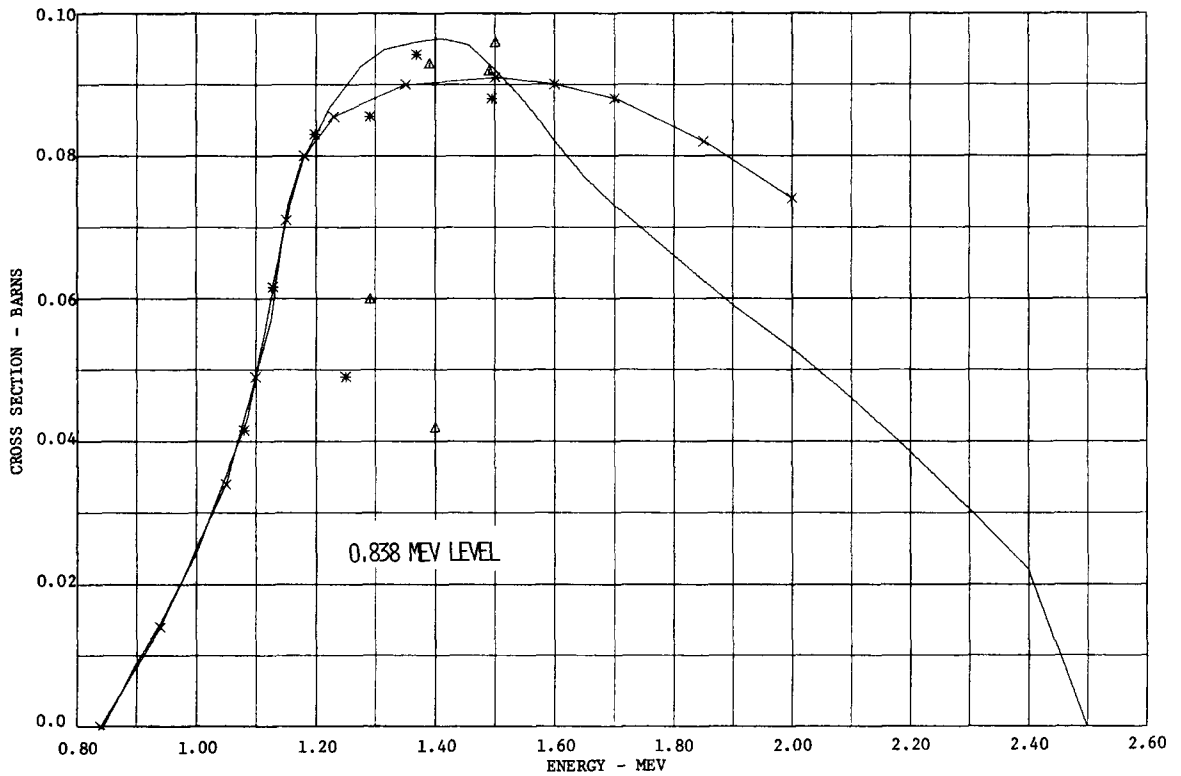
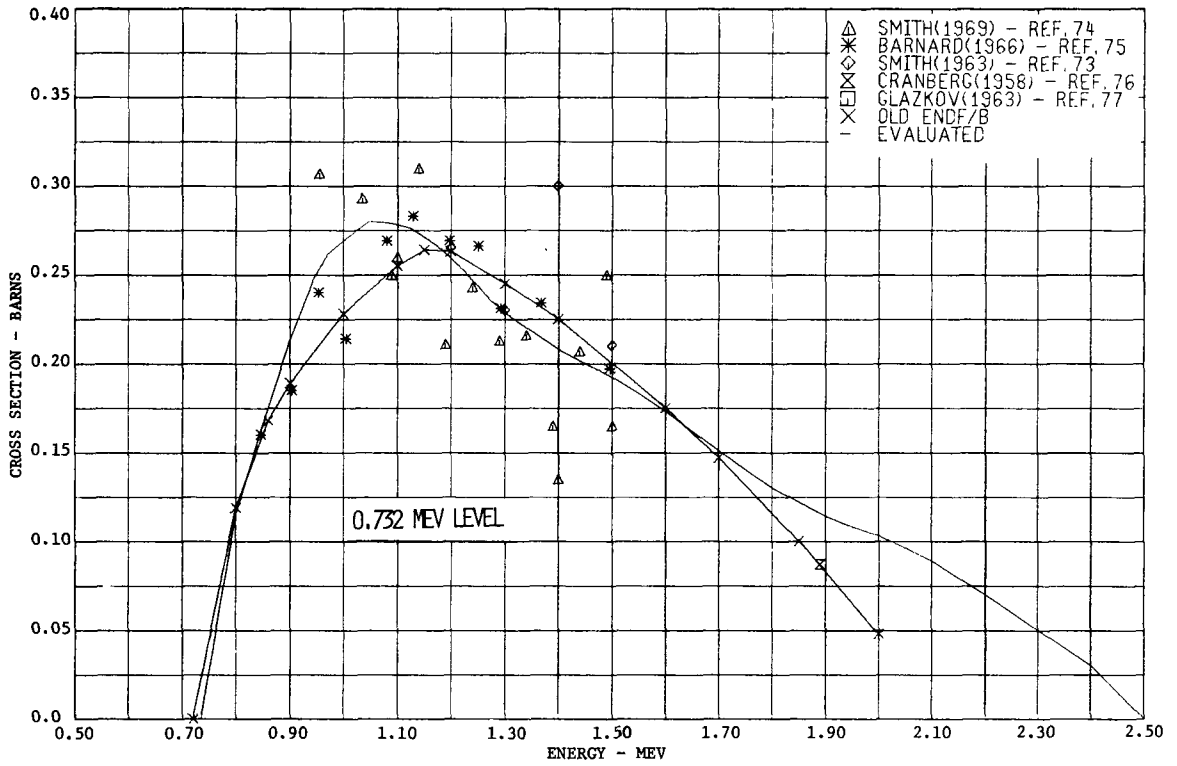


Figure 13. Inelastic Scattering Data for 0.732 and 0.838 MeV Levels

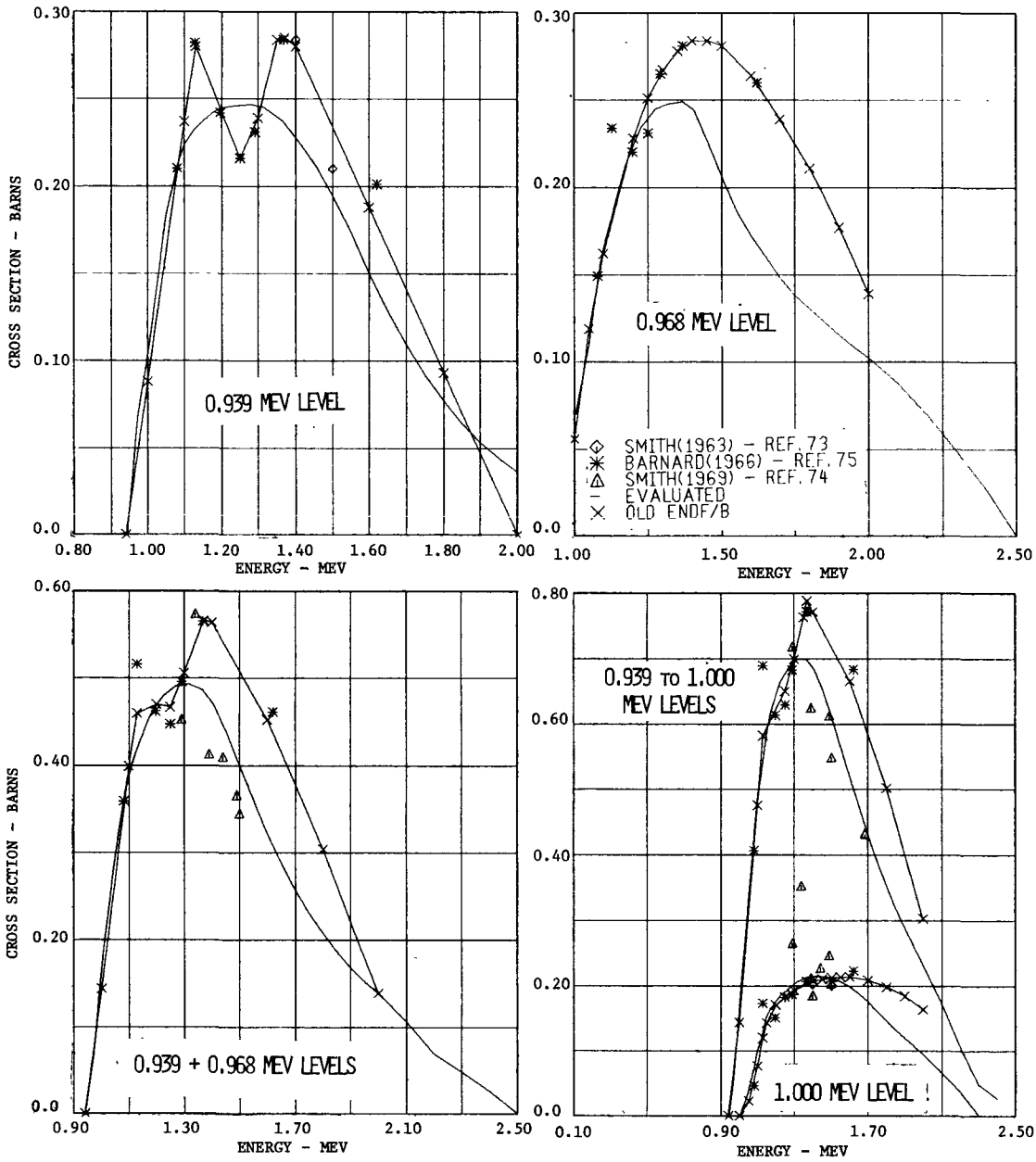


Figure 14. Inelastic Scattering Data for 0.939, 0.968 and 1.00 MeV Levels

levels compared to the 0.945 MeV level data of Smith, a comparison of Barnard's 1.006 MeV level with Smith's 0.995 MeV level, and a comparison of the sum of levels between 0.939 to 1.00 MeV for both Smith and Barnard.

Cross sections for levels at 0.939 and 0.968 MeV were evaluated based primarily on the data of Barnard while requiring that the sum of these two levels be consistent with Smith's results for a 0.945 MeV level. The resulting evaluation is shown in Figure 14 as is the evaluation for a level at 1.0 MeV.

For the sum of levels between 0.939 and 1.0 MeV, Smith measured an additional point at a neutron energy of 1.69 MeV (also shown in Figure 14). From this summation of levels, the notable discrepancy between Barnard's values at 1.62 MeV neutron energy and Smith's values between 1.5 and 1.69 MeV neutron energy can be clearly seen. A similar discrepancy can be noted for Smith's level at 0.945 MeV and the sum of Barnard's 0.939 and 0.968 MeV levels. At these higher energies, it is believed that Smith's procedure of determining the net cross section over sums of levels may be more reliable than the sums over individually determined levels by Barnard. For this reason, Smith's high energy data were more heavily weighted in the evaluation than Barnard's 1.62 MeV neutron energy data. A similar discrepancy between Barnard's 1.62 MeV points and Smith's data also exists for higher energy levels as noted below.

7. 1.045, 1.080, 1.12, 1.17 and 1.22 MeV Levels

While noting the existence of two levels at about 1.04 and 1.08 MeV, Smith [74] measured only the cross section for the sum of the two levels. Barnard measured the cross section for individual levels at 1.047 and 1.076 MeV. The experimental and evaluated data for levels at 1.045 and 1.080 as well as the sum over these two levels are shown in Figure 15. For these levels, Barnard's data are consistently higher than the measurements of Smith particular Barnard's values at 1.3 and 1.6 MeV. The evaluation is based primarily on the sum of the two levels with the distribution into the 1.045 and 1.08 MeV levels based on the relative contributions as measured by Barnard.

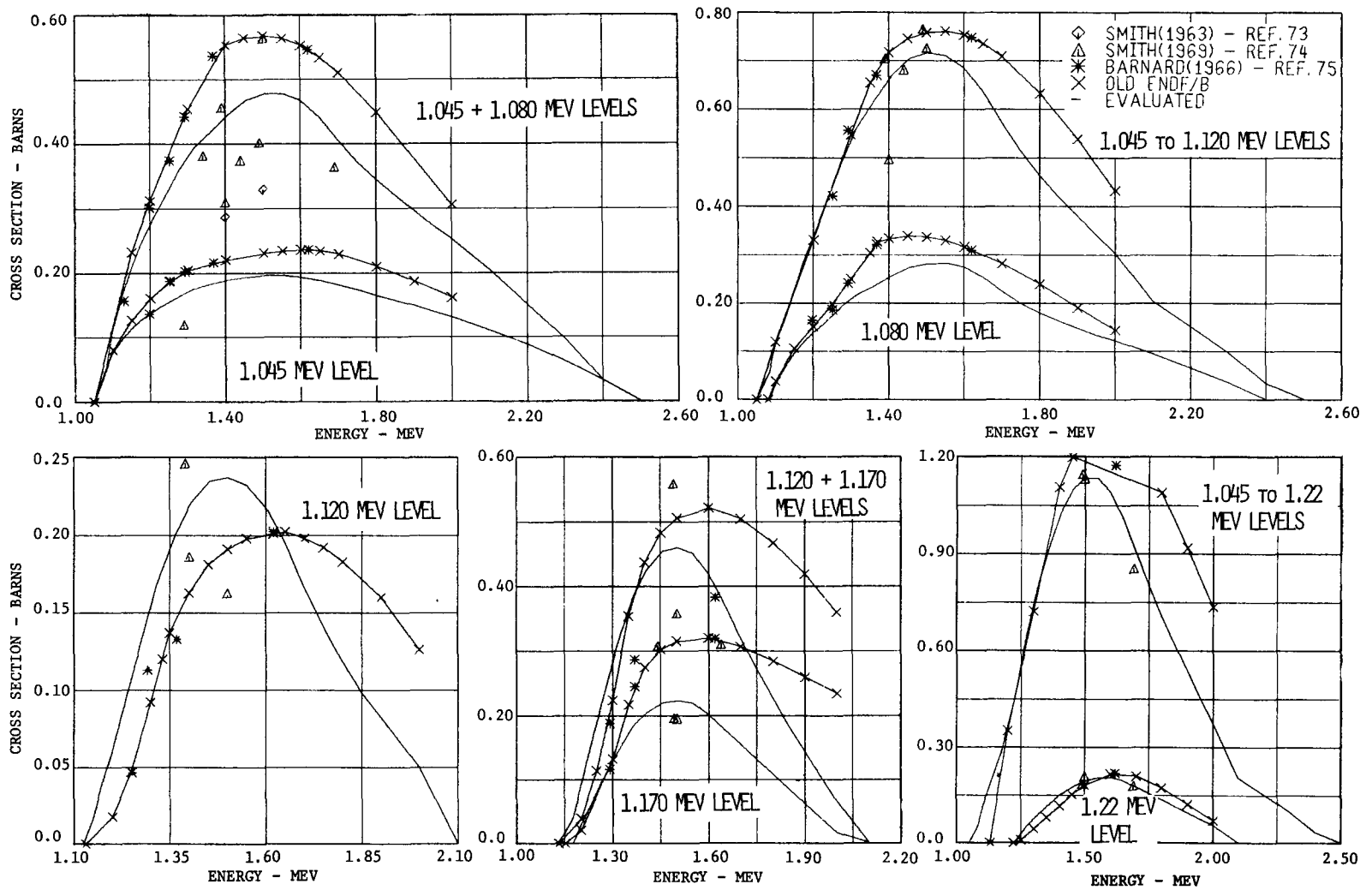


Figure 15. Inelastic Scattering Data for 1.045, 1.08, 1.12, 1.17 and 1.22 MeV Levels

The 1.115 MeV level of Smith can be compared with the 1.123 MeV level of Barnard (also given in Figure 15). For this level, Smith's results tend to be higher than Barnard's data which tend to compensate for the opposite trend for the 1.045 plus 1.08 levels. Consequently the sum of the 1.04 + 1.08 + 1.115 MeV levels of Smith is in good agreement with the sum of the 1.047 + 1.076 + 1.123 MeV levels of Barnard as compared in Figure 15.

Figure 15 compares the experimental and evaluated data for a level at 1.17 MeV based on the 1.165 MeV level of Smith and 1.15 + 1.19 MeV levels of Barnard. Also shown is a level at 1.22 MeV based on Smith's data for 1.22 MeV and the sum of Barnard's 1.21 + 1.246 MeV level data.

As a consistency check, the sum over all 5 levels between 1.045 and 1.22 MeV are compared in Figure 15. The significant discrepancy between Smith and Barnard is again the high value at 1.62 MeV obtained by Barnard.

8. 1.27, 1.31, 1.36, 1.40 and 1.45 MeV Levels

A measurement at 1.69 MeV neutron energy by Smith [74] for a level at 1.27 MeV corresponds with the sum of the 1.246 MeV and 1.272 MeV levels of Barnard and was evaluated as a 1.27 MeV level as shown in Figure 16. The additional points at 1.62 MeV neutron energy by Barnard for levels at 1.313, 1.361, 1.401, 1.437 and 1.470 MeV were evaluated at the lower limits of the uncertainty in Barnard's values as levels at 1.31, 1.36, 1.40 and 1.45 MeV as also shown in Figure 16.

C. Total Inelastic Scattering Cross Section

The total inelastic cross section up to 1.55 MeV neutron energy is treated as completely resolved and defined by the sum of 19 level cross sections. No reliable measurements of either total inelastic or non-elastic cross sections have been made below the 2.0 MeV measurements of Batchelor [64] who measured elastic scattering and inelastic scattering for excitation of levels between 0.57 and 1.38 MeV. From a total cross section of 7.45 b., Batchelor determined a non-elastic cross

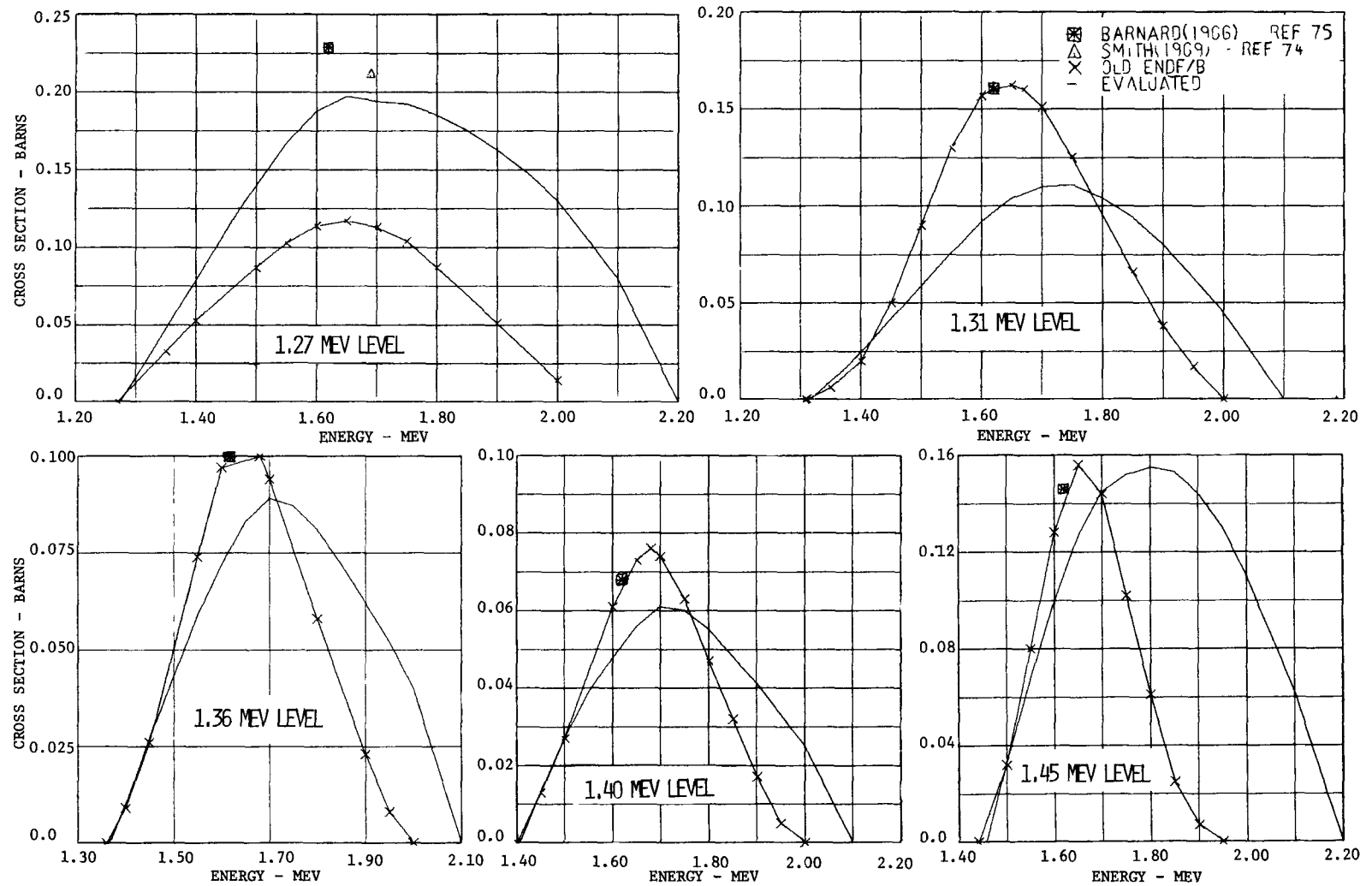


Figure 16. Inelastic Scattering Data for 1.27, 1.31, 1.36, 1.40 and 1.45 MeV Levels

section of 3.38 b. and an inelastic cross section for levels above 0.57 MeV of 2.79 b. It is not clear from Batchelor's paper [64] whether the total cross section of 7.45 b. was measured or evaluated as no uncertainties are assigned to this value. In this evaluation, nonelastic and inelastic cross sections of 3.08 b. and 2.50 b. were obtained using Batchelor's elastic scattering cross section of 4.07 ± 0.2 b. and evaluated total (7.15 b.), capture and fission cross sections. The evaluated inelastic cross section for levels above 0.57 MeV was then smoothly extrapolated (assuming the total compound reaction cross section to be nearly constant in this energy range) above 1.55 MeV to obtain a value of 2.54 b. at 2.0 MeV. With this procedure, the peak in the inelastic cross section near 1.6 MeV found in many previous ^{238}U evaluations, Reference 72 for example, is not found in this evaluation. However, the principal cause for the reduction in the peak inelastic cross section is lower weighting of the 1.62 MeV measurements of Barnard [75] in this evaluation. Above 2.00 MeV, the inelastic cross section is obtained as the difference between the evaluated nonelastic cross section and the capture, fission, (n,2n) and (n,3n) cross sections.

As noted previously, the total inelastic scattering cross section above 1.5 MeV is highly sensitive to extrapolation of the 0.045 and 0.148 MeV levels depending on assumed magnitudes of direct interaction contributions. These levels were extrapolated to zero in this evaluation at 3.0 MeV for the 0.045 MeV level and 2.75 MeV for the 0.148 MeV level.

Figure 17 compares the present evaluation and previous ENDF/B evaluation [1] (based on Schmidt [72]) for the total inelastic cross section and the cross section for excitation of levels above 0.15 MeV. The primary difference in the evaluations is the reduction in this evaluation of the high energy level excitation between 1.3 and 2.1 MeV. In addition, the 0.148 MeV level cross section is up to 20% higher between 0.9 and 1.3 MeV in the present evaluation.

D. Statistical Contribution and Nuclear Temperature

Above 1.55 MeV, the total inelastic scattering cross section is not

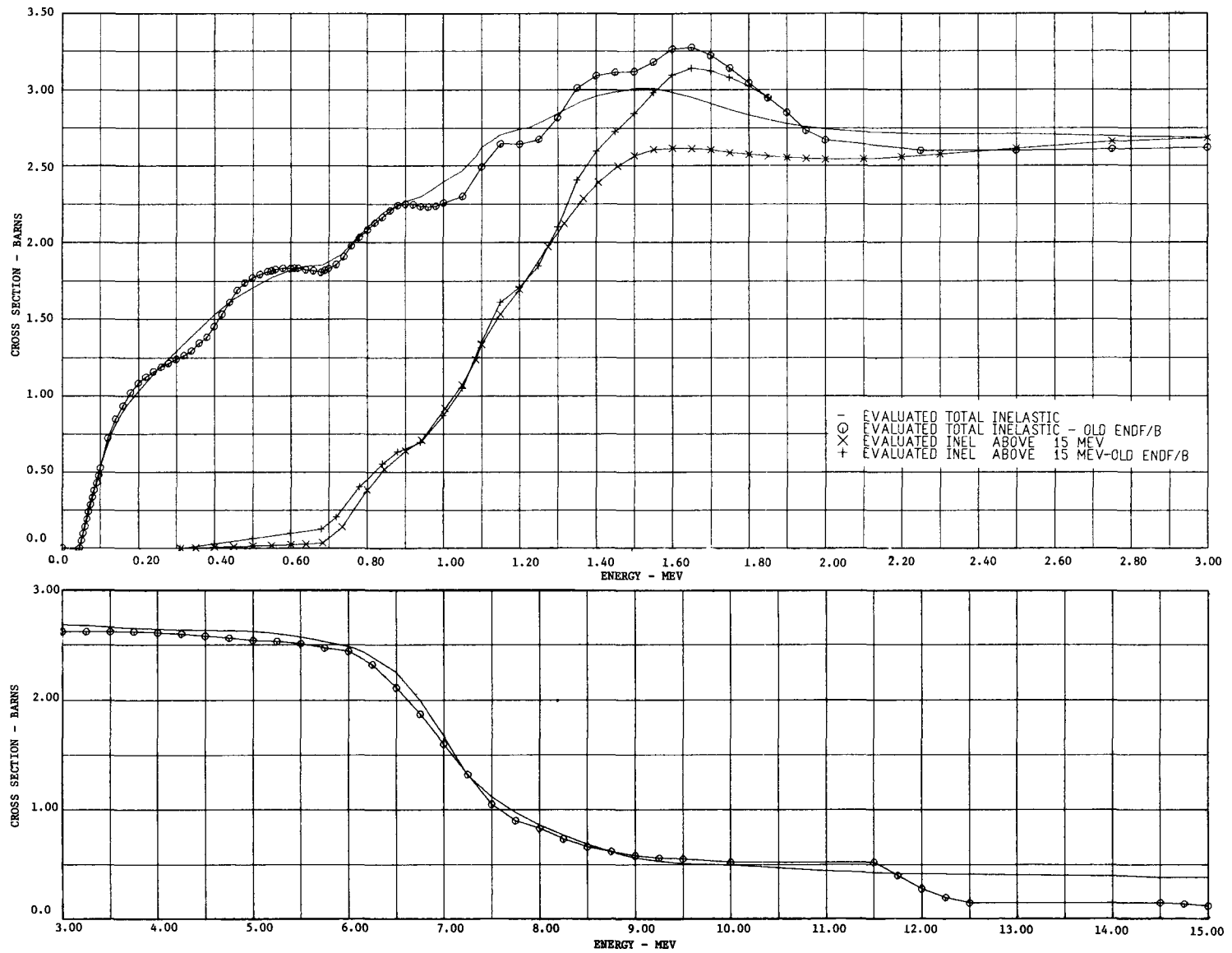


Figure 17. Comparison of Evaluated Inelastic Scattering Cross Sections

completely resolved into level assignments. The difference between the total inelastic and the sum of the resolved level cross sections was assigned to a statistical contribution represented by a Maxwellian distribution. The statistical contribution increases from zero at 1.55 MeV to be equal to the total inelastic at 3.0 MeV and higher energies.

Batchelor [64] measured the ^{238}U inelastic nuclear temperature (corrected for fission neutrons) for a Maxwellian distribution as $0.35 \pm .04$, $0.44 \pm .05$ and $0.54 \pm .06$ at 3.0, 4.0 and 7.0 MeV, respectively. These data can be fit with a nuclear temperature given by

$$T = \left(\frac{E}{a}\right)^{1/2} = 0.206 E^{1/2}$$

which was used in the present evaluation.

It can be noted that the nuclear temperature given above does not fit the resolved level distributions at 1.5 MeV or Batchelor's integral distribution measurements at 2.0 MeV. A nuclear temperature about 20% larger (therefore, a harder secondary energy distribution) would be required as noted in Section E below. However, in this evaluation, the resolved levels were extrapolated to 2.0 MeV in such a way that the sum of resolved level plus statistical contribution (using the above nuclear temperature expression) tends to predict a slightly harder secondary energy distribution than Batchelor's 2.0 MeV values.

E. Comparison of Evaluated and Measured Integral Distribution

Table 9 compares the measured cross sections for excitation of an energy band of levels with the evaluated contributions from both resolved levels and the statistical distribution. In this case, the statistical distribution was integrated over the secondary energy band yielding the same energy loss as the range of level excitations given in column 1 of the table. The present evaluation utilized liberal extrapolations of the resolved levels up to 2.5 MeV. It is seen from Table 9 that the combined resolved level excitation plus statistical distribution tends to overestimate the cross section measured by Batchelor [64] for levels below

Table 9. Comparison of Experimental and Evaluated Integral Inelastic Excitation

Range of Levels MeV	Experiment [Ref. 64]	Evaluation		
		Resolved Levels	Statistical*	Total
2 MeV				
0.57 - 0.87	0.285 ± 0.03	0.271	0.075	0.346
0.87 - 1.38	1.025 ± 0.01	0.820	0.358	1.178
1.38 - 2.00	1.19 ± 0.25 ⁺	0.135	0.828	0.963
0.57 - 2.00	2.50 ± 0.30	1.226	1.261	2.487
1.6 MeV				
0.57 - 0.87	0.37 ± 0.05	0.435	0.00	0.437
2.4 MeV				
0.57 - 0.87	0.22 ± 0.03	0.112	0.064	0.176
<p>* Statistical distribution yielding same energy loss as resolved level range</p> <p>⁺ Based on evaluated $\sigma_t = 7.15$ b of this study (see text)</p>				

1.38 MeV thus yielding a somewhat harder secondary energy distribution than Batchelor's values.

To assess the magnitude of the nuclear temperature for a statistical distribution in the vicinity of 2.0 MeV, some comparisons were made with varying nuclear temperatures compared with the evaluated secondary distribution from resolved levels at 1.5 MeV and Batchelor's 2.0 MeV values. This comparison is given in Table 10. It can be noted that the statistical distribution can be expected to reproduce only compound inelastic and would not include direct interaction contributions which

Table 10. Comparison of Experimental Integral Inelastic Excitation with Statistical Distributions

Range of Levels MeV	Experimental		Fraction of Statistical Distribution*		
	Cross Section	Fraction of Total Inelastic	T ₁ (MeV)	T ₂ (MeV)	T ₃ (MeV)
E = 2.0 MeV					
			<u>T₁ = 0.291</u>	<u>T₂ = 0.33</u>	<u>T₃ = 0.365</u>
0.00 - 0.57			0.0357	0.0542	0.0725
0.57 - 0.87	0.285 ⁺	0.114	0.0571	0.0756	0.0403
0.87 - 1.38	1.025	0.410	0.2738	0.3007	0.3171
1.38 - 2.00	1.19	0.476	0.6333	0.5696	0.5201
E = 1.5 MeV					
			<u>T₁ = 0.256</u>	<u>T₂ = 0.285</u>	<u>T₃ = 0.31</u>
0.00 - 0.57	0.485 ⁺⁺	0.161	0.1043	0.1361	0.1603
0.57 - 0.87	0.478	0.159	0.1776	0.1947	0.2083
0.87 - 1.10	1.089	0.362	0.2461	0.2468	0.2443
1.10 - 1.50	0.957	0.318	0.4720	0.4224	0.3871
<p>* Statistical distribution yielding same energy loss as resolved level range</p> <p>+ Measurements of Batchelor</p> <p>++ Evaluated from resolved levels</p>					

could be large particularly for the first two levels below 0.15 MeV. The experimental distributions of Table 10 at 1.5 MeV include direct interactions so that the percentages for levels above 0.57 MeV could be increased by a few percent for a better comparison with the statistical distributions. In general, the experimental distributions support higher nuclear temperatures in the low MeV range than the current evaluation as given in Section D above. However, unless the current evaluation significantly underestimates the excitation of levels above about 1.2 MeV (direct use of Barnard's 1.62 MeV values would only increase the cross section at 1.5 MeV for levels between 1.1 and 1.5 MeV from 0.96 to about 1.0 barn), it also appears, as might be expected, that the statistical distribution does not well represent the excitation of levels in the low MeV range.

F. Assessment of Inelastic Cross Section Accuracy

Due to the reasonable agreement of Smith [1] and Barnard [2] data (as sums over levels) below about 1.5 MeV, it can be expected that the total inelastic cross section is known to about 5% below 1.0 MeV and 8% between 1.0 and 1.5 MeV. Uncertainties on the individual level cross sections below 1.5 MeV would be larger, although levels below 1.2 MeV appear to be defined with close to 5% accuracy, except for possible fluctuations in the cross sections.

Between 1.5 MeV and 6 MeV, the total inelastic cross section for levels above 0.15 MeV is known to about 5 - 10%, although the excitation for groups of levels is less well known. In this energy range, the primary uncertainty is in the non-elastic cross section. Uncertainties in this energy range for levels below 0.15 MeV is rather large due to lack of knowledge on direct interaction considerations. However, the separation of direct excitation for these levels from elastic scattering is not particularly important for fast reactor calculations.

Between 6 and 12 MeV, the total inelastic cross section uncertainty is about 10 - 15% due to uncertainties in the non-elastic and (n,2n) cross sections. Above 12 MeV, the inelastic cross section becomes small due

to competition from (n,2n) and (n,3n) and the uncertainties could be as large as 50%.

For fast reactor calculations, measurements are needed to better define the total inelastic cross section and the secondary energy distributions between about 1.3 and 6 MeV. Since notable increases in the resolution of individual levels over this energy range is unlikely, additional measurements over groups of levels such as the Batchelor measurements could help to reduce the currently large uncertainties.

V. CONCLUSIONS

Since the present evaluation was completed, new measurements on resonance parameters, capture, total and inelastic scattering cross sections have been reported. This chapter discusses the implications of these measurements and presents estimates of the data uncertainties in the present evaluation.

A. Implications of Measurements Since Present Evaluation

New measurements on resolved parameters reported since this evaluation was completed are those of Carraro [82] for neutron widths between 66 eV and 5.7 keV, Rohr [83] for neutron and radiation widths between 66 eV and 1.05 keV and Rahn [84] for neutron and radiation widths between 6.6 eV and 1.6 keV. These measurements indicate that the large s-wave neutron widths in the present evaluation (based primarily on measurements of Garg [3]) tend to be too small by typically 5 to 10%. As a consequence, the s-wave strength function based on the new data would be about 0.95 to $1.0 \times 10^{-4} \text{ eV}^{-1/2}$ compared to $0.90 \times 10^{-4} \text{ eV}^{-1/2}$ in the present evaluation. The new measurements tend to support a radiation width close to the 23.5 value of the present evaluation.

New measurements on the capture cross section between 0 and 100 keV have been made by de Saussure [85] and between 1 keV and 0.6 MeV by Fricke [86]. The de Saussure measurements indicate capture cross sections consistently higher than the present evaluation by up to 15% below 4 keV, up to 10%

between 6 and 8 keV and about 6% between 10 and 100 keV. The reported accuracy on these measurements is better than 5%. These data can be compared with Moxon's data [19] (both measurements are relative to $B^{10}(n,\alpha)$ as used in the present evaluation which are 6 to 9% lower than the evaluated capture cross section. Both measurements are consistent on the shape of the cross section between 1 and 110 keV. Consequently, the large uncertainties in ^{238}U capture continue to exist and the present evaluation tends to be a mean of the de Saussure and Moxon data.

The capture data of Fricke [86] have about 10% accuracy. These data differ in shape below 100 keV with the well-agreeing shape of Moxon and de Saussure being lower than the Moxon data below 20 keV and in better agreement with de Saussure between 60 and 100 keV. Above 100 keV, Fricke's data indicate lower capture than the present evaluation and are in good agreement with the Menlove and Poenitz data [24]. Below 80 keV, the Fricke data are measured relative to $B^{10}(n,\alpha)$ while above 80 keV, the data are relative to the (n,p) cross section. These data thus emphasize the discrepancy above 100 keV between data measured relative to ^{235}U fission which indicate 10 to 15% higher cross sections than data relative to other standards such as Fricke [86] and Menlove and Poenitz [24] (shape measurement relative to 30 keV).

Recent measurements on the total cross section have been reported by Kopsch [87] between 0.5 and 4.35 MeV and by Cabe [88] between 0.1 and 6.0 MeV. At this time, only small graphs of the data in the papers are available and it is difficult to accurately assess the differences from the present evaluation. In general, however, it appears that these new data indicate a total cross section a few percent higher than the present evaluation.

Barnard [89] has reported new measurements for inelastic scattering up to 1.3 MeV neutron energies for the 0.0447, 0.148, 0.680 and 0.732 MeV levels. For the 0.0447 MeV level, Barnard's new data indicate a cross section about 0.3 b higher than the present evaluation. For the other levels, the new data tend to confirm the previous data and the present evaluation. However, Barnard's new data, which have relatively high resolution and energy

detail compared to previous measurements, indicate considerably more structure in the level excitation cross sections than found in previous data or the present evaluation.

B. Estimates of Data Uncertainties

Based on differences between reported measurements including the recent measurements discussed above, the following estimates of uncertainties for the data in the present evaluation are made:

1. Resonance Parameters

$$\text{Resolved } \Gamma_n \begin{matrix} +10\% \\ -5\% \end{matrix}$$

$$\langle \Gamma_\gamma \rangle = 23.5 \begin{matrix} +1.5 \\ -1.0 \end{matrix} \text{ MeV}$$

$$S_0 = 0.90 \begin{matrix} +0.1 \\ -0.03 \end{matrix} \times 10^{-4} \text{ eV}^{-1/2}$$

$$\langle D_0 \rangle = 20.8 \begin{matrix} +1.0 \\ -2.0 \end{matrix} \text{ eV}$$

$$S_1 = 2.0 \pm 0.5 \times 10^{-4} \text{ eV}^{-1/2}$$

2. Pointwise Cross Sections

$$\sigma_\gamma \quad - \begin{matrix} +15\% \\ -5\% \end{matrix} < 4 \text{ keV}, \begin{matrix} +7\% \\ - \end{matrix} 4 \text{ to } 100 \text{ keV}, \begin{matrix} +5\% \\ -15\% \end{matrix} \text{ above } 100 \text{ keV}$$

$$\sigma_f \quad - \begin{matrix} +10\% \\ -3\% \end{matrix} \text{ over entire energy range}$$

$$\sigma_{in} \quad - \begin{matrix} +8\% \\ -5\% \end{matrix} \text{ below } 1 \text{ MeV}, 5 - 10\% \text{ between } 1 \text{ and } 6 \text{ MeV}, 10-15\% \\ \text{between } 6 \text{ and } 12 \text{ MeV}, 50\% \text{ above } 12 \text{ MeV}$$

$$\sigma_t \quad - \begin{matrix} +8\% \\ -5\% \end{matrix} \text{ over entire energy range}$$

$$\sigma_{n,2n} \quad - \pm 10\% \text{ except near } 14 \text{ MeV where accuracy may be } \pm 5\%$$

$$\sigma_{n,3n} \quad - \pm 10\% \text{ over entire energy range}$$

σ_{ne} - \pm 10% between 2 and 4 MeV, 5 to 10% above 4 MeV

σ_{el} - \pm 5% below 1.5 MeV, 5 to 10% above 1.5 MeV

\bar{v} - 2 to 3%

These uncertainties in the ^{238}U data, particularly for capture and fission cross sections, do not meet the accuracy requirements of a few percent for σ_γ and σ_f that are required for reliable fast reactor analysis. The recent resonance parameter measurements in References 82 to 85 may meet fast reactor requirements on the s-wave resonance parameters below about 4 keV. Additional p-wave information between about 800 eV and 4 keV may be required for accurate predictions of the capture cross section below 4 keV.

The most important remaining data uncertainties for fast reactor analysis are:

1. Capture Cross Section Between 1 keV and About 1 MeV

Between 1 keV and 100 keV, it would appear that attempts to resolve the source of the discrepancy between Moxon [19] and de Saussure [85] might be more useful than new measurements. Above 100 keV, an accurate absolute capture measurement such as relative to (n,p) is required to clarify the presently large discrepancy between measurements relative to ^{235}U fission and the Menlove and Poenitz data [24] or the Fricke data [86].

2. Fission Cross Section

The presently evaluated fission cross section is almost certainly too low by 5 to 10% although the $^{238}\text{U}/^{235}\text{U}$ fission ratio data are quoted to 3% accuracy. Since the ^{235}U fission cross section is not well measured above 1 MeV, uncertainties in the ^{235}U fission cross section may be as important as uncertainties in the fission ratio. To resolve this discrepancy, an absolute ^{238}U fission measurement such as relative to the (n,p) cross section is required.

3. Inelastic Scattering

Based on the consistency of the Barnard [75] and Smith [74] data below about 1.2 MeV, it appears that the greatest need for new measurements is above about 1.2 to 1.5 MeV and up to about 4 MeV for fast reactor applications. Since resolution of individual level cross sections is difficult in this energy range, accurate measurements of the nonelastic cross section along with integral level excitations such as the data of Batchelor [64] would help to significantly reduce the present uncertainties.

LIST OF REFERENCES

1. W. A. Wittkopf, D. H. Roy, and A. Z. Livolsi, "²³⁸U Neutron-Cross Section Data for the ENDF/B," BAW-316, May 1967.
2. M. K. Drake, Editor, "Data Formats and Procedures for the ENDF Neutron Cross Section Library," (unpublished).
3. J. B. Garg, J. Rainwater, J. S. Petersen, and W. W. Havens, Jr., "Neutron Resonance Spectroscopy. III. Th²³² and U²³⁸," Phys. Rev. 134, pp. B985-1009 (1964)
4. J. L. Rosen, J. S. Desjardins, J. Rainwater, and W. W. Havens, Jr., "Slow Neutron Resonance Spectroscopy, I. U.²³⁸," Phys. Rev. 118, pp. 687-697 (1960).
5. F. W. K. Firk, J. E. Lynn, and M. C. Moxon, "Resonance Parameters of the Neutron Cross Section of U²³⁸," Nucl. Phys. 41, pp. 614-629 (1963).
6. M. C. Moxon, C. M. Mycock, unpublished data reported in Reference 8.
7. G. E. Thomas and L. M. Bollinger, "p-Wave Resonances in ²³⁸U at Very Low Energy," in Nuclear Structure Study With Neutrons, Proceedings of the International Conference on the Study of Nuclear Structure with Neutrons, Antwerp, July 19-23, 1965, p. 534, North-Holland Publishing Company, Amsterdam, 1966.
8. J. R. Stehn, M. D. Goldberg, Wiener-Chasman Renate, S. F. Mughabghab, B. A. Magurno, and V. A. May, "Neutron Cross Sections. Volume III. Z=88 to 98," BNL-325, 2nd ed., Suppl. 2, February 1965.
9. J. J. Schmidt, "Neutron Cross Sections for Fast Reactor Materials. Part I. Evaluation," KFK-120, February 1965.
10. M. Asghar, C. M. Chaffey, and M. C. Moxon, "Low-Energy Neutron Resonance Parameters of ²³⁸U," Nucl. Phys. 85, pp. 305-316 (1966)
11. N. W. Glass, A. D. Schelberg, L. D. Tatro, and J. H. Warren, "²³⁸U Neutron Capture Results from Bomb Source Neutrons," in Neutron Cross Sections and Technology, Proceedings of Conference, Washington, D. C., March 1968, NBS Special Publication 299, Vol. 1, pp. 573-587, 1968.
12. C. Durston, M. F. James, private communication (1970).
13. J. A. Harvey, "General Survey on Time-of-Flight Measurements Applied to Nuclear Physics," in Neutron Time-of-Flight Methods, Brussels, pp. 23-56, European Atomic Energy Community, 1961.

LIST OF REFERENCES (CONTINUED)

14. T. D. Newton, "Shell Effects on the Spacing of Nuclear Levels," Can. J. Phys. 34, No. 8, pp. 804-829 (1956); ERRATA: Can. J. Phys. 35, p. 1400 (1957)
15. B. R. Leonard, private communication (1969).
16. C. B. Bigham, R. W. Durham, and J. Ungrin, "A Direct Measurement of the Thermal Neutron Conversion Ratio of Natural Uranium," Can. J. Phys. 47, No. 12, pp. 1317-1326 (1969).
17. L. M. Bolinger, R. E. Coté, D. A. Dahlberg, and G. E. Thomas, "Neutron Resonance Structure of Uranium-238," Phys. Rev. 105, pp. 661-665 (1957).
18. W. G. Davey, "Selected Fission Cross Sections for ^{232}Th , ^{233}U , ^{234}U , ^{235}U , ^{236}U , ^{237}Np , ^{238}U , ^{239}Pu , ^{240}Pu , ^{241}Pu , and ^{242}Pu ," Nucl. Sci. Eng. 32, pp. 35-45 (1968).
19. M. C. Moxon, "The Neutron Capture Cross-Section of ^{238}U in the Energy Region 0.5 to 100 keV," AERE-R-6074.
20. W. G. Davey, "An Analysis of the Neutron Capture Cross Section of ^{238}U Between 1 KeV and 15 MeV," Nucl. Sci. Eng. 39, pp. 337-360 (1970).
21. J. F. Barry, J. Bunce, and P. H. White, "Cross Section for the Reaction $^{238}\text{U} (n,y) ^{239}\text{U}$ in the Energy Range 0.12-7.6 MeV," J. Nucl. Energy Pt. A/B 18, pp. 481-489 (1964).
22. W. P. Poenitz, "The Fission Cross-Section Ratio of ^{239}Pu and ^{235}U in the Neutron Energy Range 150 to 1400 keV," Trans. Am. Nucl. Soc. 12, No. 2, pp. 742-743 (1969).
23. W. P. Poenitz, "Measurement of the Ratios of Capture and Fission Neutron Cross Sections of ^{235}U , ^{238}U , and ^{239}Pu at 130 to 1400 keV," Nucl. Sci. Eng. 40, pp. 383-388 (1970).
24. H. O. Menlove and W. P. Poenitz, "Absolute Radiative Capture Cross Section for Fast Neutrons in ^{238}U ," Nucl. Sci. Eng. 33, pp. 24-30 (1968).
25. W. P. Poenitz, "Measurement of the U^{235} Fission Cross Section in the keV Energy Range," in Neutron Cross Sections and Technology, Proceedings of Conference, Washington, D. C., March 1968, NBS Special Publication 299, Vol. 1, pp. 503-511, 1968.

LIST OF REFERENCES (CONTINUED)

26. H. Alter and C. L. Dunford, "An Evaluation of Uranium-235 Neutron Cross Section Data for Energies Above 15 kev," AI-AEC-Memo-12916, January 1970.
27. G. de Saussure, L. W. Weston, et al, "The Measurement of α as a Function of Energy," in "Neutron Physics Division Annual Progress Report. Period Ending September 1, 1962," ORNL-3360, January 1963, pp. 51-63.
28. J. H. Gibbons, R. L. Macklin, P. D. Miller, and J. H. Neiler, "Average Radiative Capture Cross Sections for 7- to 170- kev Neutrons," Phys. Rev. 122, pp. 182-201 (1961).
29. T. S. Belanova, A. A. Van'kov, F. F. Mikhailus, and Y. Y. Stavisskii, "Absolute Measurements of the Absorption Cross Sections of 24 kev Neutrons," J. Nucl. Energy Pt. A/B 20, pp. 411-417 (1966).
30. L. B. Miller and W. P. Poenitz, "Monte Carlo Interpretation of a ^{238}U Spherical Shell Transmission Experiment at 23 keV," Nucl. Sci. Eng. 35, pp. 295-297 (1969).
31. R. L. Macklin, P. J. Pasma, and J. H. Gibbons, "Neutron Capture," in "Reports to the AEC Nuclear Cross Sections Advisory Group," WASH-1046, January 1964, p. 88-91.
32. M. C. Moxon, C. H. Chaffey, TRDWP/P8 (1966).
33. V. A. Tolstikov, L. E. Sherman, and Y. Y. Stavisskii, "A Measurement of the Capture Cross Sections of ^{238}U and ^{232}Th for 5-200 keV Neutrons," J. Nucl. Energy Pt. A/B 18, pp. 599-600 (1964).
34. R. C. Hanna and B. Rose, "Fast Neutron Capture in ^{238}U and ^{232}Th ," AERE-NP-R-1743, 1959.
35. R. W. Lamphere, "Fission Cross Sections of the Uranium Isotopes, 233, 234, 236, and 238, for Fast Neutrons," Phys. Rev. 104, pp. 1654-1660 (1956).
36. W. E. Stein, R. K. Smith, and H. L. Smith, "Relative Fission Cross Sections of ^{236}U , ^{238}U , ^{237}Np , ^{235}U ," in Neutron Cross Sections and Technology, Proceedings of Conference, Washington, D. C., March 1968, NBS Special Publication 299, Vol. 1, pp. 627-634, 1968.
37. P. H. White and G. P. Warner, "The Fission Cross Sections of ^{233}U , ^{234}U , ^{236}U , ^{238}U , ^{237}Np , ^{239}Pu , ^{240}Pu , and ^{241}Pu Relative to that

LIST OF REFERENCES (CONTINUED)

- of ^{235}U for Neutrons in the Energy Range 1-14 MeV," J. Nucl. Energy 21, pp. 671-679 (1967).
38. R. K. Smith, R. L. Henkel, and R. A. Nobles, "Neutron-Induced Fission Cross Section for U^{233} , U^{235} , U^{238} , and Pu^{239} from 2 to 10 Mev," Bull. Am. Phys. Soc. 2, pp. 196-197 (1957).
39. G. Hansen, S. McGuire, R. K. Smith, Private communication from L. Stewart (LASL) - 1969.
40. S. P. Kalinin and V. M. Pankratov, "Neutron-Induced Fission Cross Sections of Th^{232} and U^{238} in the Energy Range of 3 to 11 Mev and of U^{233} , U^{235} , Np^{237} and Pu^{239} in the Energy Range of 3 to 8 Mev," in Proceedings of the Second United Nations International Conference on the Peaceful Uses of Atomic Energy, Geneva, 1958, Vol. 16, pp. 136-140, United Nations, Geneva, 1958.
41. R. L. Henkel, "Fast Neutron Cross Sections. Corrections to LA-1714 and a Correlation of 3 MEV Values," La-2122, March 1957.
42. V. M. Pankratov, "Fission Cross Sections of ^{232}Th , ^{233}U , ^{235}U , ^{237}Np , and ^{238}U for 5-37 MeV Neutrons," J. Nucl. Energy Pt. A/B 18, pp. 215-223 (1964).
43. R. Richmond quoted by W. D. Allen and R. L. Hendel, "Fast Neutron Data on the Isotopes of Thorium, Uranium, and Plutonium," in Progress in Nuclear Energy, Series I, Volume 2, p. 29, Pergamon Press, New York, 1958.
44. R. B. Leachman and H. W. Schmitt, "The Cross-Section for U^{238} Fission by Fission Neutrons," J. Nucl. Energy 4, pp. 38-43 (1957).
45. M. N. Nikolaev, V. I. Golubev, and I. I. Bondarenko, "Fission of U^{238} ," Soviet Phys. JETP 34 (7), No. 3, pp. 517-518 (1958).
46. K. Parker, "Neutron Cross-Sections of U^{235} and U^{238} in the Energy Range 1 kev-15 Mev. Part I. Best Cross-Sections for U^{238} Based on Microscopic Experimental and Theoretical Data Available at December 1961," AWRE-O-79/63, January 1964.
47. C. A. Uttley and J. A. Phillips, "Fission Cross-Section of U^{238} , U^{235} , U^{233} , Pu^{239} , and Th^{232} for 14 Mev Neutrons," AERE-NP/R-1996, June 1956.
48. W. Nyer, "Fission Cross Sections of Thorium 232, Uranium 233, 235, and 236 and Plutonium 239 Relative to Uranium 238 for 14-Mev Neutrons," LAMS-938, June 1950.

LIST OF REFERENCES (CONTINUED)

49. G. A. Jarvis, "Fission Comparison of U^{238} and U^{235} for 2.5 Mev Neutrons," La-1571, July 1953.
50. B. Adams, R. Batchelor, and T. S. Green, "The Energy Dependence of the Fission Cross-Sections of ^{238}U , ^{235}U , and ^{239}Pu for Neutrons in the Energy Range 12.6 to 20 MeV," J. Nucl. Energy, Pt. A/B, Reactor Sci. Technol. 14, pp. 85-90 (1961).
51. J. D. Knight, R. K. Smith, and B. Warren, " $U^{238}(n,2n)U^{237}$ Cross Section from 6 to 10 Mev," Phys. Rev. 112, pp. 259-261 (1958).
52. Graves, Conner, Ford, Warren, unpublished, quoted by Knight.
53. D. Barr, unpublished (1966), private communication L. Stewart (1969).
54. D. S. Mather and L. F. Pain, "Measurement of (n,2n) and (n, 3n) Cross Sections at 14-MeV Incident Energy," AWRE-0-47/69, August 1969.
55. K. J. LeCouteur, "Statistical Fluctuations in Nuclear Evaporation," Proc. Phys. Soc. (London) A65, pp. 718-737 (1952).
56. M. Drake, et.al., private communication (Nov. 1969).
57. M. Soleilhac, J. Frehaut, and J. Gauriau, "Energy Dependence of $\bar{\nu}_p$ for Neutron-Induced Fission of ^{235}U , ^{238}U , and ^{239}Pu from 1.3 to 15 MeV," J. Nucl. Energy 23, pp. 257-282 (1969).
58. G. C. Hanna, C. H. Westcott, H. D. Lemmel, B. R. Leonard, Jr., J. S. Story, and P. M. Attree, "Revision of Values for the 2200 m/s Neutron Constants for Four Fissile Nuclides," Atomic Energy Review 7, No. 4, pp. 3-92.
59. C. A. Uttley, Private communication (1967).
60. J. Whalen, Private communication A. B. Smith (1965).
61. D. G. Foster, unpublished.
62. R. L. Henkel, L. Cranberg, G. A. Jarvis, R. Nobles, and J. E. Perry, Jr., "Total Neutron Cross Section for Uranium from 20 KeV to 20 MeV," Phys. Rev. 94, pp. 141-143 (1954).
63. A. Bratenahl, J. M. Peterson, and J. P. Stoering, "Neutron Total Cross Sections in the 7 to 14 MeV Region," Phys. Rev. 110, pp. 927-936 (1958).

LIST OF REFERENCES (CONTINUED)

64. R. Batchelor, W. B. Gilboy, and J. H. Towle, "Neutron Interactions with U^{238} and Th^{232} in the Energy Region 1.6 Mev to 7 Mev," Nucl. Phys. 65, pp. 236-256 (1965).
65. A. V. Cohen, "The Non-Elastic Neutron Cross-Section for Uranium at 13-19 MeV and Beryllium at 14 MeV," J. Nucl. Energy, Pt. A/B, Reactor Sci. and Technol. 14, pp. 180-185 (1961).
66. P. P. Lebedev, Y. A. Zysin, Y. S. Klintsov, and B. D. Stsiborskii, "Neutron Yield in Inelastic Collisions of 14-m.e.v. Neutrons with Nuclei and Cross Section for the (n, 2n) Reaction," Soviet J. At. Energy 5, pp. 1431-1434 (1958).
67. J. Kirkbride, "Two Supplements to Report A.E.R.E. NP/R 2086. 1. A Redetermination of the Total Inelastic Cross Section of Natural Uranium for 14 MEV Neutrons. II. A Determination of the Total Inelastic Cross Section of Natural Uranium for Neutrons of Energies from 4 to 14 MEV," AERE-NP/R-2086, Suppl. 1 and 2, 1957.
68. Y. G. Degtyarev and V. G. Nadtochii, "Measurement of the Inelastic Interaction Cross Section of 13 to 20 MEV Neutrons for Certain Isotopes," Soviet J. At. Energy 11, pp. 1043-1044 (1962).
69. H. A. Bethe, J. R. Beyster, and R. E. Carter, "Inelastic Cross Sections and $\bar{\nu}$ for Some Fissionable Isotopes," LA-1939, August 1955.
70. LA-1142 - D. D. Phillips (1950).
71. Rice Institute, unpublished, quoted in LA-1939 (1960).
72. J. J. Schmidt, KFK-120, February 1966.
73. A. B. Smith, "Scattering of Fast Neutrons from Natural Uranium," Nucl. Phys. 47, pp. 633-651 (1963).
74. A. B. Smith, Private Communication (1969).
75. E. Barnard, A. T. G. Ferguson, W. R. McMurray, and I. J. Van Heerden, "Scattering of Fast Neutrons by ^{238}U ," Nucl. Phys. 80, pp. 46-64 (1966).
76. L. Cranberg and J. S. Levin, "Inelastic Neutron Scattering by U^{238} ," Phys. Rev. 109, pp. 2063-2070 (1958).
77. N. P. Glazkov, "Inelastic Neutron Scattering Spectra and Cross Sections of U, Th, Hg, W, Sb, Cd, Mo, Nb, and Fe Nuclei in the 0.2 to 1.2-Mev Range," At. Energ. 14, pp. 400-402 (1963).

LIST OF REFERENCES (CONTINUED)

78. C. L. Dunford, "Evaluation of Heavy Even-Even Nuclide Elastic and Inelastic Cross-Sections by Means of a Non-Spherical Optical Model," in Nuclear Data for Reactors, Proceedings of a Conference on Nuclear Data-Microscopic Cross-Sections and Other Data Basic for Reactors, Paris, October 17-21, 1966, Vol. I, pp. 429-443, International Atomic Energy Agency, Vienna, 1967.
79. G. Prince, Private communication (1969).
80. J. Terrell, "Neutron Yields from Individual Fission Fragments," Phys. Rev. 127, pp. 880-904 (1962).
81. EANDC (UK) - 35L - C. A. Uttley (1964).
82. G. Carraro and W. Kolar, "Neutron Widths of ^{238}U from 60 eV to 5.7 keV," in Nuclear Data for Reactors, Proceedings of the Second International Conference on Nuclear Data for Reactors, Helsinki, June 15-19, 1970, Vol. I, pp. 403-412, International Atomic Energy Agency, Vienna, 1970.
83. G. Rohr, H. Weigmann, and J. Winter, "Resonance Parameters from Neutron Radiative Capture in ^{238}U ," in Nuclear Data for Reactors, Proceedings of the Second International Conference on Nuclear Data for Reactors, Helsinki, June 15-19, 1970, Vol. I, pp. 413-417, International Atomic Energy Agency, Vienna, 1970.
84. F. J. Rahn, Columbia University, Private Communication.
85. G. de Saussure, Oak Ridge National Laboratory, Private Communication.
86. M. P. Fricke, W. M. Lopez, S. J. Friesenhahn, A. D. Carlson, and D. G. Costello, "Measurements of Cross-Sections for the Radiative Capture of 1-keV to 1-MeV Neutrons by Mo, Rh, Gd, Ta, W, Re, Au, and ^{238}U ," in Nuclear Data for Reactors, Proceedings of the Second International Conference on Nuclear Data for Reactors, Helsinki, June 15-19, 1970, Volume II, pp. 265-280, International Atomic Energy Agency, Vienna, 1970.
87. D. Kopsch, S. Cierjacks, and G. J. Kirouac, "New Total Neutron Cross-Section Measurement of Uranium Between 0.5-4.35 MeV," in Nuclear Data for Reactors, Proceedings of the Second International Conference on Nuclear Data for Reactors, Helsinki, June 15-19, 1970, Vol. II, pp. 39-49, International Atomic Energy Agency, Vienna, 1970.
88. J. Cabe, M. Cance, A. Adma, M. Beaufour, and M. Labat, "Mesure des Sections Efficaces Totales Neutroniques du Carbone, du Nickel, de l'Uranium-235, del'Uranium'238 et du Plutonium-239 entre 0.1 MeV et 6 MeV," in Nuclear Data for Reactors, Proceedings of the Second International Conference on Nuclear Data for Reactors, Helsinki,

LIST OF REFERENCES (CONTINUED)

- June 15-19, 1970, Vol. II. pp. 31-37, International Atomic Energy Agency, Vienna, 1970.
89. E. Barnard, J. A. M. DeVilliers, and D. Reitmann, "Inelastic Scattering of Fast Neutrons from ^{238}U ," in Nuclear Data for Reactors, Proceedings of the Second International Conference on Nuclear Data for Reactors, Helsinki, June 15-19, 1970, Vol. II, pp. 103-107, International Atomic Energy Agency, Vienna, 1970.
90. H. H. Barschall, (unpublished).
91. M. H. MacGregor, R. Booth, and W. P. Ball, "Nonelastic Neutron Cross-Section Measurements on Li^6 , Li^7 , U^{235} , U^{238} , and Pu^{239} at 8.1, 11.9, and 14.1 Mev," PHYS. REV. 130, pp. 1471-1472 (1963).
92. Y. G. Degtyarev, "Cross Sections for Neutron Inelastic Interactions with ^7Li , ^{12}C , ^{14}N , ^{27}Al , ^{56}Fe , Cu, Pb, ^{235}U , ^{238}U , and ^{239}Pu ," At. Energ. 19, pp. 456-457 (1965).
93. J. R. Beyster, M. Walt, and E. W. Salmi, "Interaction of 1.0-, 1.77-, 2.5-, 3.25-, and 7.0-MEV Neutrons with Nuclei," Phys. Rev. 104, pp. 1319-1331 (1956).
94. H. A. Bethe, J. R. Beyster, and R. E. Carter, "Inelastic Cross Sections and ν for Some Fissionable Isotopes," LA-1939, August 1955.
95. D. Didier, H. Dillemann, P. Thouvenin, and E. Fort, "Mesure des Sections non Elastiques par la Methode de la Couche Spherique," in "Progress Report on Nuclear Data Research in the Euratom Community," EANDC (E)-49 (L), October 1963, pp. 85-86.